

# The default network and the combination of cognitive processes that mediate self-generated thought

Vadim Axelrod<sup>1,2\*</sup>, Geraint Rees<sup>2,3</sup> and Moshe Bar<sup>1</sup>

**Self-generated cognitions, such as recalling personal memories or empathizing with others, are ubiquitous and essential for our lives. Such internal mental processing is ascribed to the default mode network—a large network of the human brain—although the underlying neural and cognitive mechanisms remain poorly understood. Here, we tested the hypothesis that our mental experience is mediated by a combination of activities of multiple cognitive processes. Our study included four functional magnetic resonance imaging experiments with the same participants and a wide range of cognitive tasks, as well as an analytical approach that afforded the identification of cognitive processes during self-generated cognition. We showed that several cognitive processes functioned simultaneously during self-generated mental activity. The processes had specific and localized neural representations, suggesting that they support different aspects of internal processing. Overall, we demonstrate that internally directed experience may be achieved by pooling over multiple cognitive processes.**

Self-generated cognition (also referred to as internally directed cognition or internal processing), such as recalling memories, thinking about the future or just mind wandering, is a key part of our experience. The functional roles and benefits of self-generated thinking are not fully understood<sup>1</sup>, but given the abundance of this type of thinking in our lives<sup>2</sup>, self-generated thinking is likely to be essential for humans. Accordingly, understanding the cognitive and neural mechanisms of self-generated cognition is an important endeavour. The literature on self-generated cognition<sup>3,4</sup> makes a distinction between self-generated processing that is initiated by an external task (for example, when a participant is asked to recall some specific past episode<sup>5–8</sup>) and spontaneous, unconstrained self-generated processing without a specific task (for example, mind-wandering<sup>9–12</sup>). In the present study, we explore task-initiated self-generated processing.

It is generally accepted that the default mode network (DMN) is the principal brain locus of internal processing and self-generated cognition<sup>4,13–16</sup>. The DMN has been implicated in various types of processing, such as self-referential processing<sup>17–25</sup>, mental scene construction<sup>25–28</sup> and scene imagery<sup>29</sup>, mental time travel<sup>30–32</sup>, semantic processing<sup>33–36</sup>, constructive episodic memory<sup>5,6</sup> and retrieval of episodic memory<sup>37–42</sup>, social-related processing<sup>43–49</sup>, affective and emotional processing<sup>50</sup>, and creativity<sup>51,52</sup>. In addition, functional heterogeneity within the DMN has been established<sup>53–65</sup>. A conceptualization of these and similar observations has been provided by the multi-component account, according to which the DMN operates through multiple interactive components (or cognitive processes) working together<sup>4</sup>. While the authors of this account do not specify this explicitly, the two important functional principles that stem from the multi-component account are (1) different cognitive processes work at the same time and (2) different cognitive processes are responsible for specific and distinct types of processing. Accordingly, to directly and empirically support the multi-component account, both principles must be shown in action within the same experiment. Previous research on self-generated

cognition using both task-based experiments<sup>7,8,21,66–74</sup> and spontaneous (for example, resting scan) experiments<sup>36,75–82</sup> showed that different parts of the DMN and connectivity between different DMN nodes are selective to different tasks and types of processing. These results have generally supported the multi-component account. Notably, none of the previous studies (except for one; see below) showed different processes working at the same time. In addition, in many task-based studies, the cognitive processes were not identified specifically because this was not the goal of these studies. The only study that satisfied conditions of direct support has been the study of Andrews-Hanna and colleagues<sup>83</sup>, which used a combination of resting-state hierarchical clustering, future and present self-related decision tasks, and behavioural introspective measures. The authors showed that the DMN consists of three functionally distinct subsystems that are active at the same time. It is noteworthy that specifically identifying cognitive processes has been traditionally challenging because the cognitive processes are inherently intertwined during self-generated processing. For example, recalling a past episode is likely to entail both episodic memory retrieval and mental scene construction processing, but to tease these two processes apart experimentally is not straightforward<sup>28,84</sup>. Additional examples of non-easily dissociated processes include mental time travel and scene construction<sup>25,83,85</sup>, episodic memory retrieval and self-referential processing<sup>18,86</sup>, and episodic and semantic memory<sup>87–90</sup>. In the present study, we devised an approach to address the aforementioned challenges and limitations. This approach permitted us to comprehensively and systematically characterize cognitive processing within the DMN during self-generated processing and to test the multi-component proposal directly.

Thirty-six participants took part in four functional magnetic resonance imaging (fMRI) experiments (thirty-one of whom took part in all four experiments). Experiment 1 was the principal self-generated experiment, which included 15 s blocks of free retrieval of personal episodic memory, future and past imagery, and an empathizing task. Experiments 2–4 selectively manipulated specific

<sup>1</sup>Gonda Multidisciplinary Brain Research Center, Bar Ilan University, Ramat Gan, Israel. <sup>2</sup>Institute of Cognitive Neuroscience, University College London, London, UK. <sup>3</sup>Wellcome Trust Centre for Neuroimaging, University College London, London, UK. \*e-mail: [vadim.axelrod@gmail.com](mailto:vadim.axelrod@gmail.com)

cognitive processes: experiment 2 was a self-referential experiment with visually presented verbs that characterize a person; experiment 3 visually presented images of scenes and objects; and experiment 4 visually presented meaningful sentences and non-words (that is, it involved language-related processing). We predicted that the execution of the self-generated, free tasks in experiment 1 would be associated with the activity of different cognitive processes. Our approach was to use experiments 2–4 to manipulate specific cognitive processes selectively and then to use the activity of each of these experiments to identify corresponding cognitive processes during the self-generated processing in experiment 1. Our goal was to identify and delineate three specific cognitive processes (that is, self-referential, mental scene construction and language-related processing) and to show the functioning of these processes at the same time during internal processing, thus supporting the hypothesis that mental experience is mediated by different cognitive processes. It should be emphasized that the goal of the present study was not to determine differences between individual internal tasks; therefore, the comparison of individual tasks was performed only when it served our main goal (see above).

## Results

**Experiment 1: self-generated cognition.** While lying in the scanner, participants were asked to generate mental experiences associated with a given picture (Fig. 1a). Four tasks of interest were used: imagine what happened before ('past imagery') or after ('future imagery') the depicted scene, recall a personal episodic memory related to the depicted scene ('episodic memory') or imagine yourself as the person in the picture ('empathizing'). The baseline condition was the generation of rhymes for a given word. The structure of the trials and visual stimuli were the same for all five conditions, including irrelevant image presentation in the baseline condition to preserve equivalent visual stimulation (see Methods for more details). The four tasks of interest are hereafter referred to as 'internal mentation' or 'internal' tasks. At the end of each trial, participants provided vividness ratings of their internal experience (Fig. 1a). The scale ranged from 1 (highest vividness) to 4 (lowest vividness). Vividness ratings were as follows: episodic memory (mean = 1.74, s.e.m. = 0.07), future imagery (mean = 1.74, s.e.m. = 0.07), past imagery (mean = 1.92, s.e.m. = 0.07) and empathizing (mean = 1.77, s.e.m. = 0.08). Conditions varied with regard to the level of vividness (one-way repeated measures analysis of variance:  $F_{3,105} = 3.67$ ,  $P = 0.015$ , effect size partial  $\eta^2 = 0.095$ ). This effect was due to a lower vividness in past imagery compared with the other three conditions.

To examine the activity associated with each of the four internal mentation tasks, each task was contrasted separately with the rhyme-generation baseline condition (four separate contrasts; random effects, group-level analysis; primary voxel-wise threshold  $P < 0.001$ ; cluster-level threshold  $P < 0.05$ , corrected; the primary threshold  $P < 0.001$  has previously been shown to control well for the false positive rate<sup>90,91</sup>). The group-level results are shown in Fig. 1b. All four contrasts (that is, internal tasks) yielded typical DMN activations<sup>13</sup>, thus confirming previous reports that different types of internal mental activity engage the DMN<sup>66,92</sup>. As the next step, for key nodes of the DMN network, we extracted percent signal change time-courses. The regions of interest (ROIs) (Fig. 1c and Supplementary Table 1) were independently defined<sup>93</sup> based on the individual DMN activation maps obtained in the first session of our experiment; all the analyses presented below were conducted using the remaining sessions (see Methods and Supplementary Methods for more details). The time courses for all conditions are shown in Fig. 2. First, in all ROIs, we identified a dissociation between the four internal mentation tasks and the baseline rhyme-generation task (average of four internal tasks versus baseline task:  $t_{35} > 7.68$ ,  $P < 5 \times 10^{-9}$ ). It is worth noting that in both internal and baseline

conditions the participants had their eyes closed. Thus, the robust dissociation between two types of conditions underscores that activation of the DMN reflects not merely the absence of an external task, but is also dependent on the nature of the non-external task (for example, episodic memory thinking versus rhyme generation). Second, the shape of the internal tasks' time courses differed across DMN regions. In particular, we observed a clear, positive, inverted U-shape response in the posterior cingulate cortex (PCC) and angular gyrus, as well as in the medial prefrontal cortex (mPFC) in the episodic memory condition. In contrast, there was a negative U-shape response in the parahippocampal cortex (PHC). Dissociation between DMN regions hints at different roles played by different regions in internal processing. It is noteworthy that from the activation maps (Fig. 1b), we could not discern whether the response to the task of interest was activation (for example, PCC and angular gyrus) or deactivation (for example, PHC). Finally, in the PCC and mPFC, there were visibly higher responses in the episodic memory condition compared with the other conditions. A plausible explanation for this effect is that episodic memory (that is, recalling of personal events) entailed stronger self-related processing compared with other tasks<sup>86</sup>. This hypothesis is corroborated by the results in this text (see, Supplementary Fig. 2a), but in general, the dissociation between internal tasks is not the focus of the present paper.

We thus established that the DMN was activated by all of the internal tasks of experiment 1. Next, we proceeded with our main goal—namely, to demonstrate that self-generated processing in the DMN operates through several independent processes.

**Experiment 2: self-referential processing.** We used a commonly accepted method to elucidate self-referential processing by contrasting the activity resulting from making a judgment about the self versus someone else<sup>94–96</sup>. In our experiment, participants made two types of judgment for the same verbs that describe a person (the 'self-referential' condition; that is, whether an action was characteristic of them; and the 'non-self-referential' condition; that is, whether an action was characteristic of some ideal person; see Methods for more details). To validate the effectiveness of our manipulation, after the experiment, participants rated their subjective experience during the experiment by answering "To what extent was each of the tasks associated with self-related and personal thoughts?" on a Likert scale from 1 (low) to 10 (high). The results confirmed that the self-referential condition was associated with more self-related and personal thoughts than the non-self-referential condition ('self-referential': mean = 6.03, s.e.m. = 0.517; 'non-self-referential': mean = 4.45, s.e.m. = 0.489; paired, two-sided  $t$ -test:  $t_{30} = 5.09$ ,  $P < 0.001$ , Cohen's  $d = 0.95$ , confidence interval (CI): 0.94 to 2.21).

First, we conducted a general linear model (GLM) second-level, random-effect analysis contrasting the 'self-referential' versus 'non-self-referential' conditions (Fig. 3a). In all figures, the blue contour denotes the DMN identified using first session (independent) data. In agreement with previous reports<sup>96</sup>, most of the activations were found in the DMN medial frontal, posterior cingulate and left lateral posterior parietal regions. This provides evidence, albeit indirect, that during self-generated internal tasks these parts of the DMN are engaged in self-referential processing.

To obtain more direct evidence, we conducted a representational similarity analysis<sup>97</sup> between experiments 1 and 2. Compared with spatial activation overlap, representational similarity analysis provides stronger evidence because they inform us about the similarity of information processing in brain regions<sup>98,99</sup>. For each participant and within each ROI (across voxels), we correlated between contrast values of internal processing selectivity (experiment 1; contrast: episodic memory + past imagery + future imagery + empathizing > rhymes generation) and contrast values of self-referential selectivity (experiment 2; contrast: 'self-referential' > 'non-self-referential').

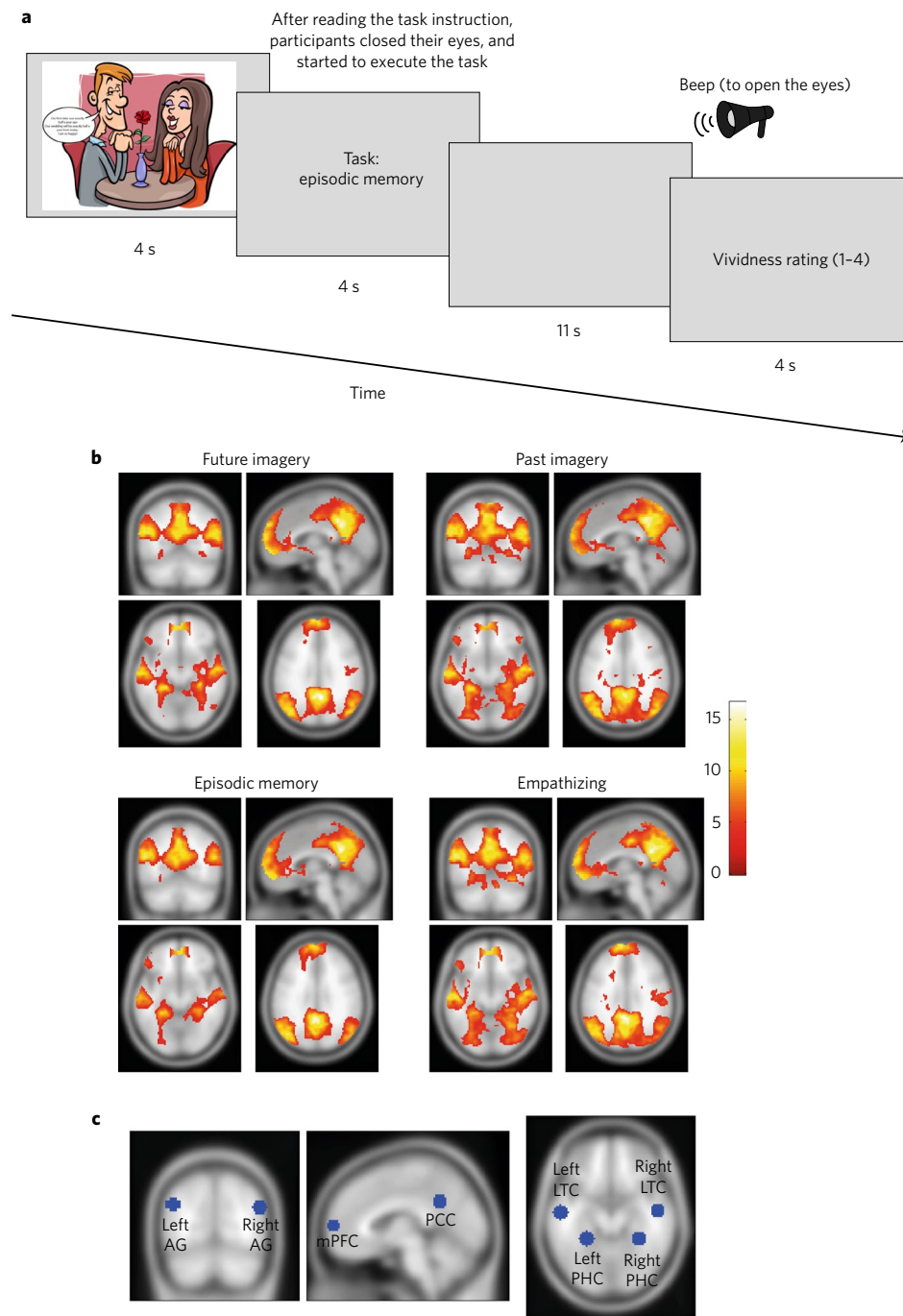


**Fig. 1 | Experiment 1: schematic flow of the experimental trial, results of the group-level analysis of four internal tasks and location of the ROIs.**

**a**, Schematic flow of the trial (from left to right). After seeing a picture, the participants received the task instruction and started to execute the task with their eyes closed. The task execution ended with a beep sound, followed by a vividness rating of the experience. There were five tasks (conditions): imagine what happened before (past imagery) or after (future imagery) the depicted scene, recall a personal episodic memory related to the depicted scene (episodic memory) and imagine yourself in the place of the person in the image (empathizing). The baseline condition was to generate words that rhymed with a provided word (the target word was provided at the stage of task instruction). Each of the pictures was repeated once for each of the five experimental conditions. Notably, the image was presented in all conditions, including baseline, to preserve identical visual stimulation. Accordingly, the contrast between internal task and baseline does not include the activity elicited by the visual scene. The text within speech balloon of this specific stimulus was: "Our first date was exactly half a year ago. Our wedding will be exactly half a year from today. I am so happy!". Note, that images of the real-life situation used in the experiment were real images, not cartoons as shown here. Real picture not shown here due to copyright restrictions. **b**, Results of the group-level random effect analysis of experiment 1 ( $n = 36$ ). Four tasks of interest (episodic memory, future imagery, past imagery and empathizing) contrasted separately against the rhyme-generation baseline task (primary voxel-wise threshold  $P < 0.001$ ; cluster-level threshold  $P < 0.05$ , corrected). Note the typical DMN activations for all four conditions. Statistical maps were overlaid on a T1 SPM template brain. Colour scale:  $t$ -values of  $T$ -contrast. **c**, Average location of the ROIs. The ROIs used in the analysis were defined as individual clusters and were not spherical (see Methods). The locations here represent the average location across participants (see also Supplementary Table 1). AG, angular gyrus; LTC, lateral temporal cortex; mPFC, medial prefrontal cortex; PCC, posterior cingulate cortex; PHC, parahippocampal cortex. Credit for cartoon in **a**: Zoonar GmbH / Alamy Stock Photo.

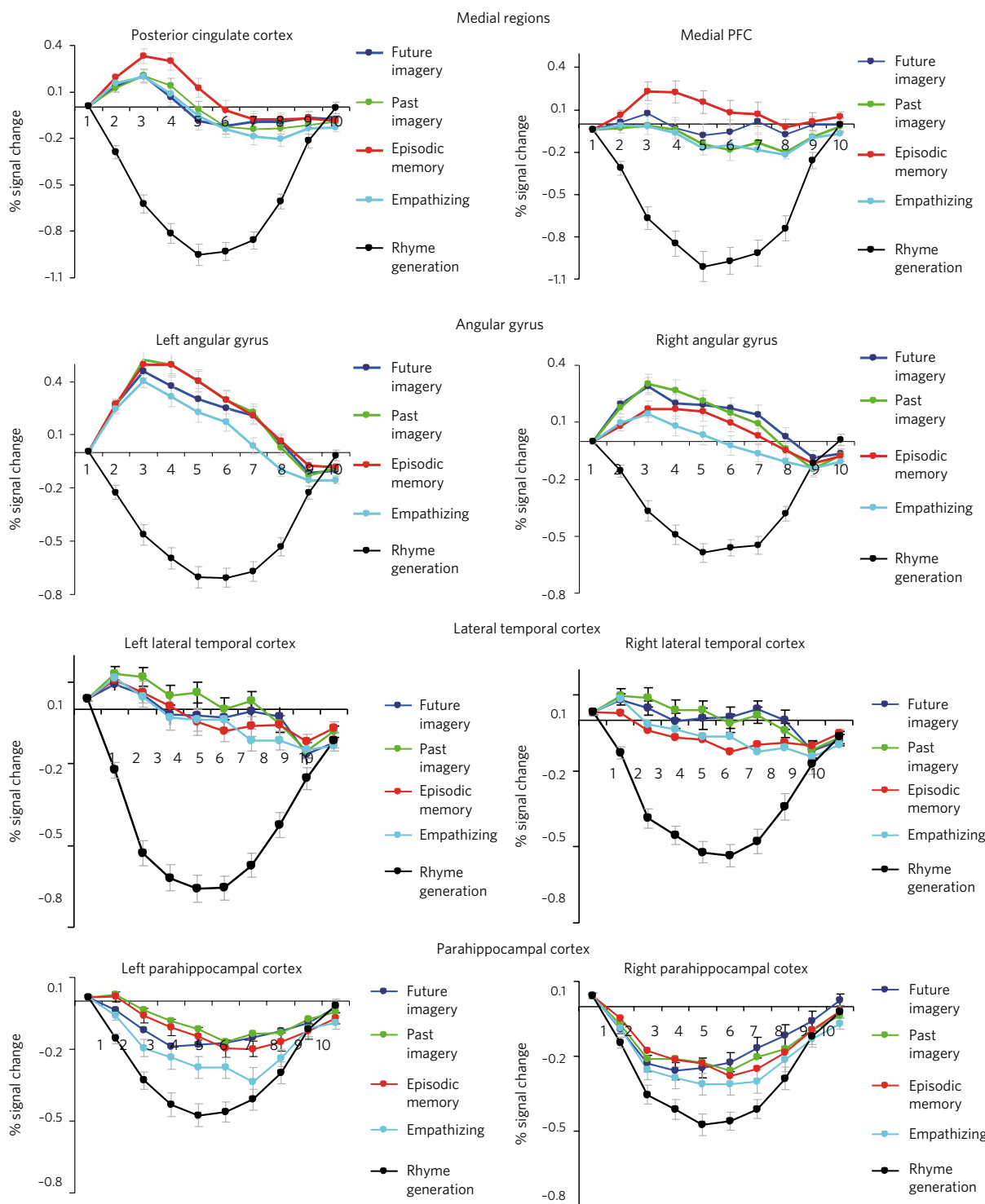


**Fig. 2 | Experiment 1 (n = 36): percent signal-change time courses for the five experimental conditions in the DMN.** The units of the x axis show repetition times (2.5 s). The first bin of the x axis corresponds to the onset of task instruction (see Fig. 1a). The error bars represent s.e.m. Note (1) the large differences between the four internal tasks and the rhyme-generation baseline condition, (2) the differences in the shapes of the time courses across the internal tasks (a clear positive and inverted U-shape response in the PCC, angular gyrus and mPFC in the episodic memory condition and a clear negative and U-shape response in the PHC) and (3) the higher response to episodic memory compared with other internal tasks in the mPFC and PCC.

The results of this analysis are shown in Fig. 3b (for individual data, see Supplementary Fig. 1a). Similarity between the two experiments was significantly above zero (after multiple comparison Bonferroni correction for the number of tested regions,  $n=8$ ,  $\alpha=0.05/8=0.00625$ ) in mPFC ( $t_{33}=6.37$ ,  $P<0.001$ , Cohen's

$d=1.09$ , 99.375% CI: 0.22 to 0.61), PCC ( $t_{33}=4.75$ ,  $P<0.001$ , Cohen's  $d=0.81$ , 99.375% CI: 0.14 to 0.57) and left angular gyrus ( $t_{33}=3.82$ ,  $P<0.001$ , Cohen's  $d=0.65$ , 99.375% CI: 0.07 to 0.5). In the left lateral temporal cortex (LTC), the similarity was above zero, but did not reach significance after multiple comparison

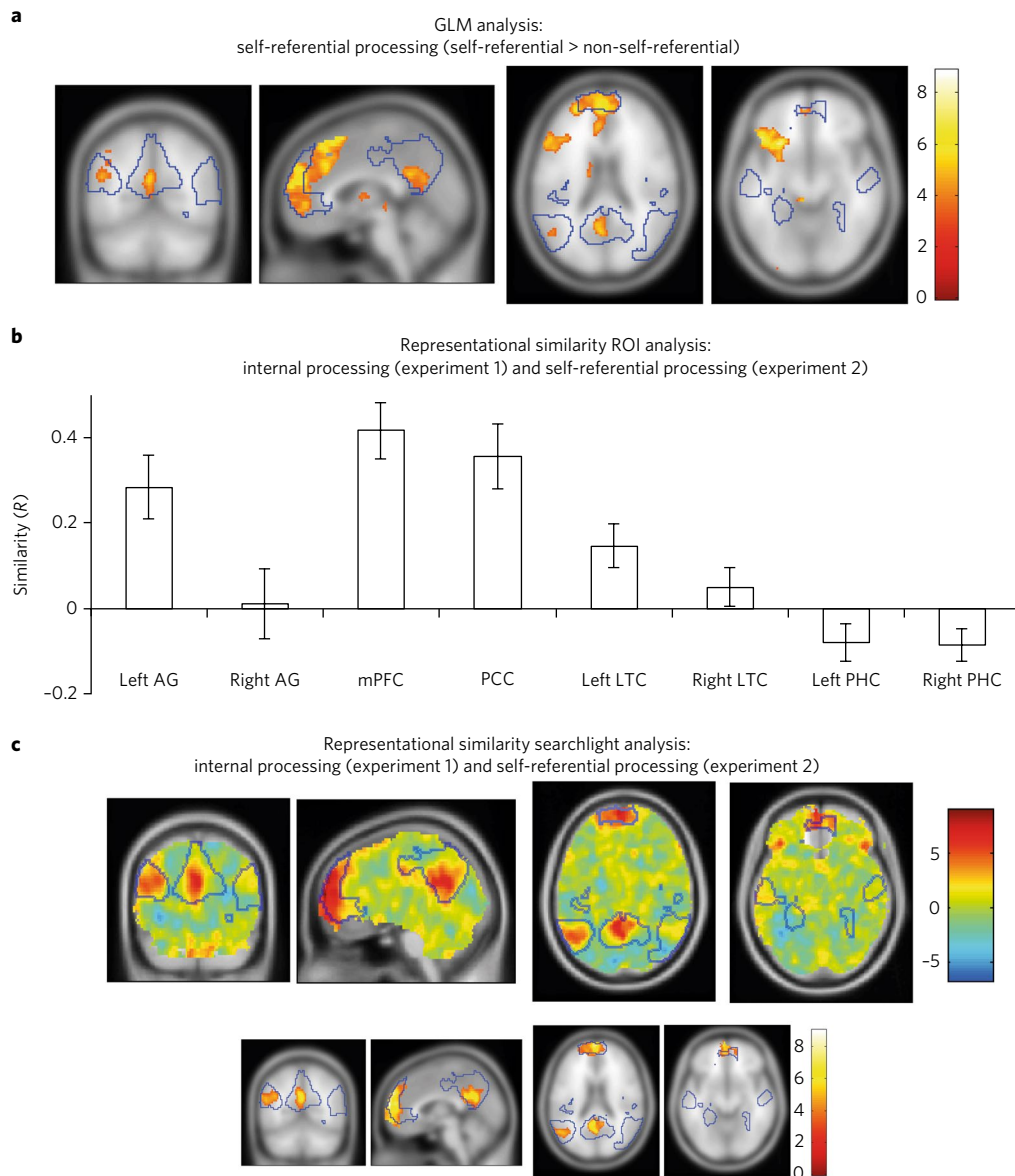


**Fig. 3 | Experiment 2 ( $n = 34$ ): self-referential processing. a**, Group-level random effect analysis of self-referential processing in experiment 2 (contrast: 'self-referential' > 'non-self-referential'). Statistical threshold: primary voxel-wise threshold  $P < 0.001$ ; cluster-level threshold  $P < 0.05$ , corrected. The blue contour line denotes the DMN identified using the first (independent) session of the experiment (four internal conditions > baseline). Note that significant clusters within the DMN were found in the mPFC, PCC and left angular gyrus, but not in the PHC, LTC and right angular gyrus. **b**, ROI representational similarity analysis between internal processing (experiment 1, four internal tasks combined) and self-referential processing (experiment 2). The values reflect the average across participants within-ROI Spearman correlation between the internal processing contrast of experiment 1 (four internal tasks > baseline) and the self-referential processing contrast of experiment 2 ('self-referential' > 'non-self-referential'). Similarity values denote Fischer z-transformed correlation results. Note the high similarity values in the mPFC, PCC and, to a lesser extent, left angular gyrus. Significance above zero was established using a one-sample, two-tailed  $t$ -test (multiple comparison Bonferroni correction for the number of tested regions,  $n = 8$ ,  $\alpha = 0.05/8 = 0.00625$ ). For regional-specificity and task-specificity analyses, see the Results. The error bars represent s.e.m. For individual data, see Supplementary Fig. 1a. **c**, Searchlight ROI representational similarity analysis between internal processing (experiment 1, four internal tasks combined) and self-referential processing (experiment 2). Top: unthresholded statistical results map. Bottom: thresholded significant clusters (primary voxel-wise threshold  $P < 0.001$ ; cluster-level threshold  $P < 0.05$ , corrected). Note the high similarity in the mPFC, PCC and left posterior parietal cortex, but not in other regions of the cortex. Also note the strong left lateralization in the posterior parietal cortex. Colour scales:  $t$ -values of T-contrast.

( $t_{33} = 2.83$ ,  $P = 0.0078$ , Cohen's  $d = 0.49$ , 99.375% CI:  $-0.004$  to  $0.3$ ). In the remaining regions, the similarity did not differ from zero ( $t < 1$ ). To examine the specificity of the result, we conducted two types of analysis. First, we tested regional specificity by comparing the similarity between regions. For the mPFC and PCC, the similarity was significantly higher (after multiple comparison Bonferroni correction for the number of tested regions,  $n = 7$ ,  $\alpha = 0.05/7 = 0.0071$ )

than in the right angular gyrus, bilateral LTC and bilateral PHC ( $P < 0.001$ , Cohen's  $d > 0.6$ ). For the left angular gyrus, the similarity was significantly higher than in the right angular gyrus, right LTC and bilateral PHC ( $P < 0.001$ , Cohen's  $d > 0.71$ ), but did not significantly differ from the left LTC after multiple comparison correction ( $P = 0.021$ , Cohen's  $d > 0.42$ ). No significant difference in similarity was observed between the mPFC, PCC and left angular gyrus

( $P > 0.1$ ). Second, we tested processing type specificity by comparing the similarity obtained in the present analysis (that is, similarity between experiment 1: internal processing and experiment 2: self-referential processing) versus the similarity of experiment 1: internal processing and each of two additional experiments presented below (experiment 3: scene construction and experiment 4: language-related processing; see Supplementary Methods for more details). Compared with internal processing versus scene construction, we found high specificity in the mPFC ( $t_{31} = 5.5$ ,  $P < 0.001$ , Cohen's  $d = 1$ ), PCC ( $t_{31} = 4.96$ ,  $P < 0.001$ , Cohen's  $d = 0.92$ , 99.375% CI: 0.35 to 0.76) and left angular gyrus ( $t_{31} = 4.26$ ,  $P < 0.001$ , Cohen's  $d = 0.75$ , 99.375% CI: 0.17 to 0.86). Compared with internal processing versus language-related processing, there was high self-referential specificity in the mPFC ( $t_{31} = 3.89$ ,  $P < 0.001$ , Cohen's  $d = 0.69$ , 99.375% CI: 0.11 to 0.82) and PCC ( $t_{31} = 2.87$ ,  $P = 0.007$ , Cohen's  $d = 0.51$ , 99.375% CI:  $-0.001$  to 0.6), but not in the left angular gyrus ( $t_{31} < 1$ ).

In addition to ROI analysis, we conducted a searchlight representational similarity analysis between internal processing (experiment 1) and self-referential selectivity (experiment 2). The main benefit of this approach is that this analysis makes no a priori assumptions regarding ROI location, thus permitting the examination of similarity across different parts of the DMN, as well as outside the DMN. The unthresholded findings are shown in the top row of images in Fig. 3c and the significant clusters are shown in the bottom row of images in Fig. 3c (primary voxel-wise threshold  $P < 0.001$ ; cluster-level threshold  $P < 0.05$ , corrected). Remarkably, in line with ROI analysis, the only significant clusters were in the mPFC, PCC and left angular gyrus (Supplementary Table 2). We can clearly see that no significant representational similarity was identified (at the statistical thresholds used) in the LTC, PHC or right angular gyrus DMN regions or any outside-DMN regions. Taken together, we conclude that the mPFC, PCC and left angular gyrus were the primary loci of self-referential processing during internal processing in experiment 1.

In previous analyses, the four internal tasks were considered as one condition (that is, 'internal processing'). As a complementary and more exploratory analysis, we conducted a representational similarity analysis between the individual internal tasks of experiment 1 and experiment 2 (for full results, see Supplementary Results, 'Representational ROI analysis of individual tasks'). In the mPFC and PCC, across the four tasks of experiment 1, the highest similarity was observed between the episodic memory task and the self-referential processing of experiment 2 (Supplementary Fig. 2a). This result corroborates the idea that higher blood oxygen-level dependent (BOLD) signals associated with episodic memory in the mPFC and PCC of experiment 1 (Fig. 2) were at least partially related to self-referential processing.

In a complementary analysis, we also tested similarities between self-referential and language-related processing (experiment 3), as well as the similarity between self-referential and scene-construction processing (experiment 4). The results of these analyses are presented in the Supplementary Results and Supplementary Figs. 3 and 4. We found clusters with high similarity between self-referential and language-related processing in the lateral temporal and frontal cortex, but mostly not within the DMN (Supplementary Fig. 4).

**Experiment 3: scene construction.** The results of experiments 1 and 2 reveal an interesting dissociation with regard to the PHC: whereas this region exhibited a much higher response to internal tasks compared with the baseline in experiment 1 (Figs. 1b and 2), it was not involved in self-referential processing in experiment 2 (Fig. 3). In general, the PHC has primarily been implicated in spatial navigation, visual scene processing and contextual processing<sup>100</sup>. In addition, it has been suggested that the region plays a role in scene construction during internal mentation<sup>25–28</sup>, as well as in imagery<sup>29</sup>. To test whether the scene construction hypothesis can explain the dissociation between experiments 1 and 2

with regard to PHC, after the study we asked participants to rate the extent to which each of the tasks was associated with them having a mental scene in their minds. A Likert scale was used: 1 (low)–10 (high). We found that in experiment 1, the subjective experience of 'a scene in the mind' was much stronger during the internal tasks than during the rhymes generation task (internal tasks: mean = 7.74, s.e.m. = 0.33; rhymes generation: mean = 1.52, s.e.m. = 0.21;  $t_{32} = 19.33$ ,  $P < 0.001$ , Cohen's  $d = 3.36$ , CI: 5.57 to 6.88). In contrast, in experiment 2 there was only a slight and insignificant difference in the subjective experience of a scene in the mind between the 'self-referential' and 'non-self-referential' conditions ('self-referential': mean = 3.16, s.e.m. = 0.43; 'non-self-referential': mean = 2.8, s.e.m. = 0.44;  $t_{30} < 1$ , Cohen's  $d = 0.17$ , CI:  $-0.39$  to 1.09). Thus, the role of the PHC during internal processing of experiment 1 may indeed be related to mental scene construction. To investigate this question more directly, we conducted an additional fMRI experiment with the same participants. Experiment 3 included visual presentation of unfamiliar images of scenes and objects<sup>101</sup>. The key idea was to use the scene-selective activity of experiment 3 as the neural marker to find mental scene construction during the self-generated tasks of experiment 1.

First, we conducted a GLM second-level, random-effect analysis contrasting 'scenes' versus 'objects' conditions (Fig. 4a). This revealed a well-characterized network of scene-selective regions in the PHC, retrosplenial cortex and middle occipital gyrus (also referred as transverse occipital sulcus)<sup>102</sup>. Large parts of this network overlapped with the DMN (particularly the PHC), but there were also parts of the network identified outside the DMN (in line with a recent report<sup>103</sup>). Thus, the fact that the same neural substrates were active in both experiments 1 and 3 supports, albeit indirectly, the idea that scene construction processes may play a role during internal processing in experiment 1.

Next, using the same independent ROIs defined in experiment 1, we conducted a representational similarity analysis between internal processing in experiment 1 and scene construction in experiment 3. The results are shown in Fig. 4b (for individual data, see Supplementary Fig. 1b). We found that the only two regions that showed strong and highly significant positive similarity (after multiple comparison Bonferroni correction for the number of regions) were the left PHC ( $t_{32} = 6.74$ ,  $P < 0.001$ , Cohen's  $d = 1.17$ , 99.375% CI: 0.14 to 0.37) and right PHC ( $t_{32} = 7.09$ ,  $P < 0.001$ , Cohen's  $d = 1.23$ , 99.375% CI: 0.15 to 0.36). In all remaining regions, the similarity was negative. This result was close to significance (after multiple comparison correction) only in the PCC ( $t_{32} = -2.92$ ,  $P = 0.0062$ , Cohen's  $d = 0.51$ , 99.375% CI:  $-0.45$  to 0), but not in other regions ( $P > 0.01$ , Cohen's  $d < 0.47$ ). Examination of a direct regional specificity revealed that similarity in the bilateral PHC was significantly higher (after multiple comparison correction) than in all other regions ( $t_{32} > 4.01$ ,  $P < 0.001$ , Cohen's  $d > 0.89$ ). Examination of processing type specificity revealed high specificity in the bilateral PHC relative to internal processing versus self-referential processing (left PHC:  $t_{31} = 5.06$ ,  $P < 0.001$ , Cohen's  $d = 0.89$ , 99.375% CI: 0.16 to 0.51; right PHC:  $t_{31} = 5.5$ ,  $P < 0.001$ , Cohen's  $d = 0.97$ , 99.375% CI: 0.16 to 0.47). Relative to internal processing versus sentence-related processing, we found high specificity in the right PHC ( $t_{31} = 4.16$ ,  $P < 0.001$ , Cohen's  $d = 0.74$ , 99.375% CI: 0.07 to 0.39) and moderate specificity in the left PHC ( $t_{31} = 2.41$ ,  $P = 0.022$ , Cohen's  $d = 0.43$ , 99.375% CI:  $-0.03$  to 0.3).

In addition, we conducted a searchlight representational analysis between internal processing (experiment 1) and scene construction (experiment 3). The results are shown in Fig. 4c. In line with ROI analysis, the highest similarity was found in the bilateral PHC (Supplementary Table 2). In addition, we found relatively high levels of similarity in the retrosplenial cortex and middle occipital gyrus. In line with ROI representational analysis, we can see strong negative similarity (light blue) in the medial frontal and posterior cortex, as well as in the left posterior parietal DMN regions (Fig. 4c, top).

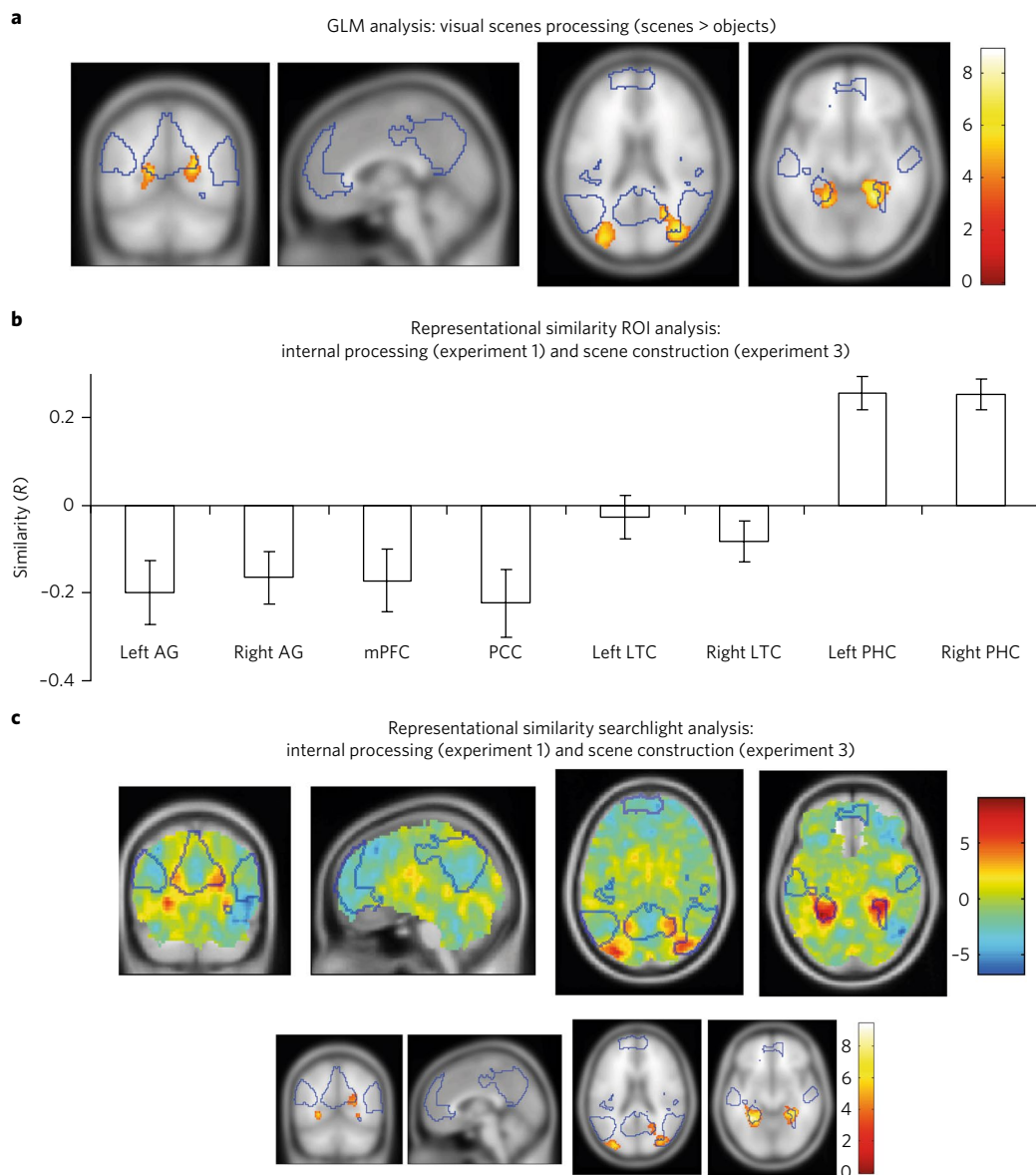


**Fig. 4 | Experiment 3 ( $n = 33$ ): scene construction. a**, Group-level random effect analysis of the scenes > objects contrast. Statistical threshold: primary voxel-wise threshold  $P < 0.001$ ; cluster-level threshold  $P < 0.05$ , corrected. Note that the largest and most significant clusters within the DMN were found in the PHC. **b**, ROI representational similarity analysis between internal processing (experiment 1, four internal tasks combined) and the scenes > objects contrast (experiment 3). Note the much higher than zero similarity values in the bilateral PHC. Significance above zero was established using a one-sample, two-tailed  $t$ -test (multiple comparison Bonferroni correction for the number of tested regions,  $n = 8$ ,  $\alpha = 0.05/8 = 0.00625$ ). The error bars represent s.e.m. For individual data, see Supplementary Fig. 1b. **c**, Searchlight ROI representational similarity analysis between internal processing (experiment 1, four internal tasks combined) and the scenes > objects contrast (experiment 3). Top: unthresholded statistical results map. Bottom: thresholded significant clusters (primary voxel-wise threshold  $P < 0.001$ ; cluster-level threshold  $P < 0.05$ , corrected). Note the high similarity in the PHC and, to a lesser extent, in the retrosplenial cortex and middle occipital gyrus, but not in other regions of the cortex. Colour scales:  $t$ -values of  $T$ -contrast.

Taken together—and in agreement with the literature on scene construction<sup>25–28</sup>—we conclude that (1) scene construction processing is likely playing an active role during internal mentation processing and (2) the PHC and, to a lesser extent, parts of the retrosplenial cortex and middle occipital gyrus are the loci of scene construction processing during internal mentation.

As in experiment 2, we also conducted exploratory a representational similarity analysis in the PHC between the individual internal tasks of experiment 1 and experiment 3 (see Supplementary Results, ‘Representational ROI analysis of individual tasks’). The similarity level across individual internal tasks was mostly similar, with a slight trend to lower similarity in the empathizing task.

**Experiment 4: language-related processing.** Language processing activates a large extent of the lateral parietotemporal and frontal lobes<sup>104,105</sup>. The language network partially overlaps with the DMN (that is, LTC and lateral posterior cortex regions), although specifically in the domain of language research, spatial overlap with the DMN has drawn relatively little attention<sup>104,106–108</sup> (but see refs<sup>109,110</sup>). In addition, there is a broad concept of semantic processing, which is explored both as part of the language system<sup>111</sup> and as an independent domain (for example, conceptual knowledge<sup>112</sup> or semantic information about a face<sup>113,114</sup>). Following the seminal work of Binder et al.<sup>33</sup>, the role of semantics in DMN processing is widely acknowledged. While early work tended to suggest the involvement of the whole DMN in

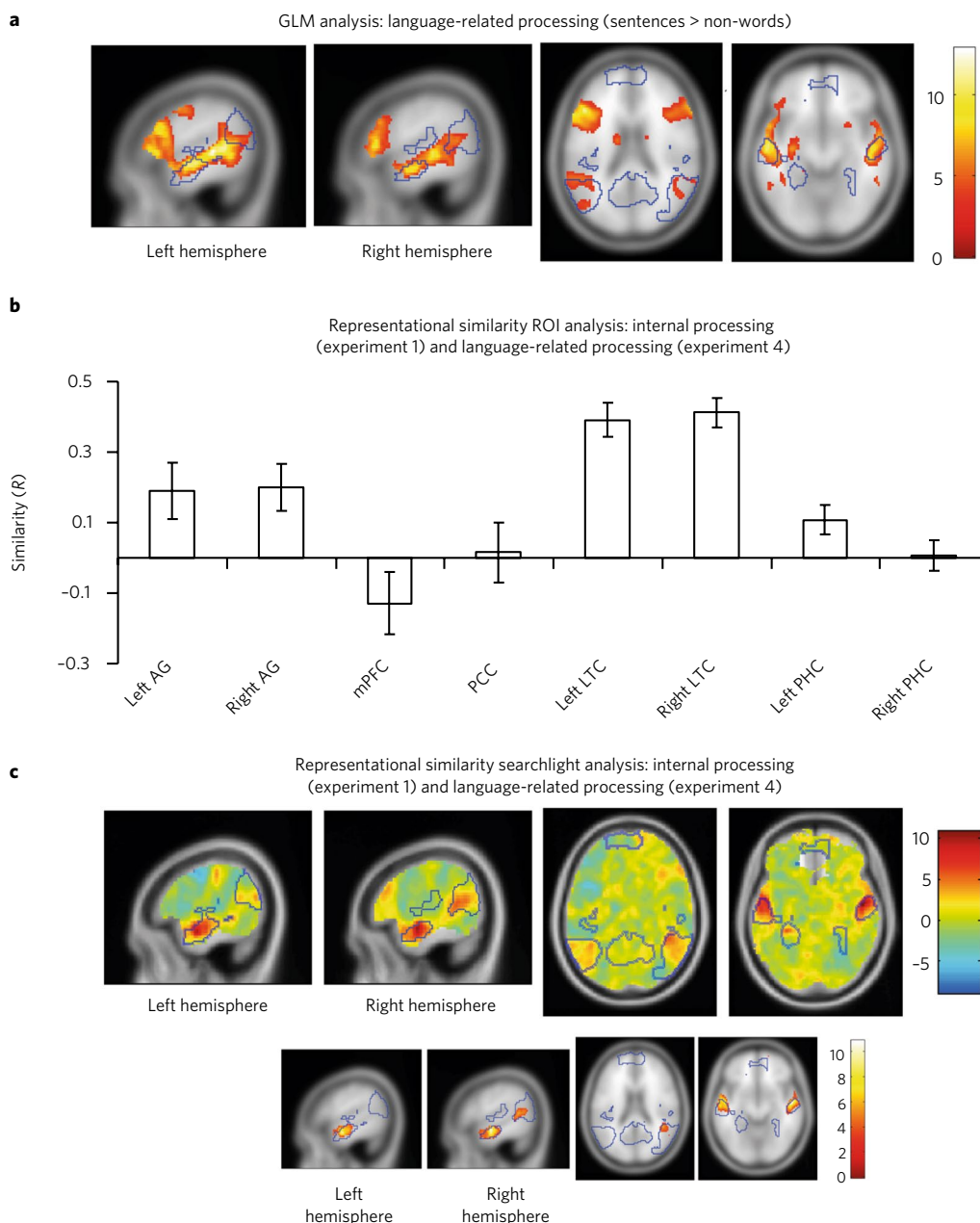


**Fig. 5 | Experiment 4 ( $n = 34$ ): language-related processing.** **a**, Group-level random effect analysis of language-related processing in experiment 4 (contrast: meaningful sentences > meaningless non-words). Statistical threshold: primary voxel-wise threshold  $P < 0.001$ ; cluster-level threshold  $P < 0.05$ , corrected. Note that the largest and most significant clusters within the DMN were found in the LTC. **b**, ROI representational similarity analysis between internal processing (experiment 1, four internal tasks combined) and language-related processing (meaningful sentences > meaningless non-words, experiment 4). Note the highest similarity values in the bilateral LTC. Significance above zero was established using a one-sample, two-tailed  $t$ -test (multiple comparison Bonferroni correction for the number of tested regions,  $n = 8$ ,  $\alpha = 0.05/8 = 0.00625$ ). The error bars represent s.e.m. For individual data, see Supplementary Fig. 1c. **c**, Searchlight ROI representational similarity analysis between internal processing (experiment 1, four internal tasks combined) and language-related processing (meaningful sentences > meaningless non-words, experiment 4). Top: unthresholded statistical results map. Bottom: thresholded significant clusters (primary voxel-wise threshold  $P < 0.001$ ; cluster-level threshold  $P < 0.05$ , corrected). Note the highest similarity in the bilateral LTC. Colour scales:  $t$ -values of  $T$ -contrast.

semantic processing<sup>33,115</sup>, more recent studies have emphasized the role of more specific DMN nodes, such as the LTC and lateral posterior cortex<sup>34,35,116</sup> and, to a lesser extent, the PCC<sup>117</sup>. We used our general approach described above to identify language-related processing during internal processing (that is, the internal tasks of experiment 1). The same participants of experiments 1–3 took part in experiment 4, which used a well-established paradigm to identify language-related processing<sup>105</sup>. Participants were visually presented with meaningful sentences

and series of meaningless non-words, while the words or non-words were presented one item at a time (see Methods for full details).

First, we conducted a GLM second-level, random-effects analysis contrasting meaningful sentences and meaningless non-word conditions (Fig. 5a). We observed a well-known network of regions related to language processing<sup>105</sup>. We could also clearly see that the bilateral LTC and, to lesser extent, lateral posterior cortex regions overlapped with the DMN. Next, using independent

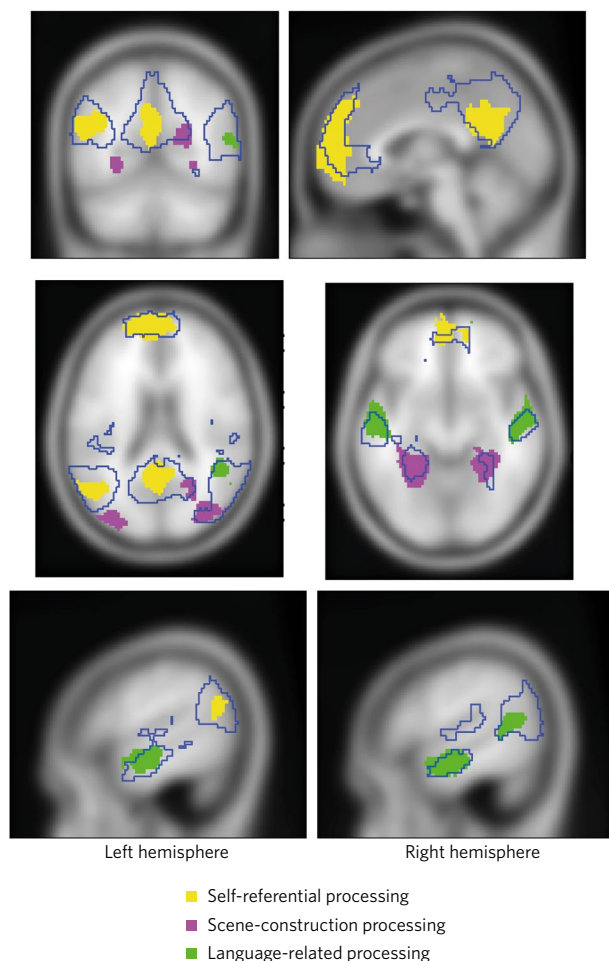


**Fig. 6 | Summary results: neural loci of three cognitive processes.**

The results reflect thresholded and binarized maps of corresponding searchlight representational analyses (Figs. 3c, 4c and 5c). The three cognitive processes are self-referential processing (yellow), mental scene construction (magenta) and language-related processing (green). Note that cognitive systems had specific loci (that is, there was no spatial overlap between cognitive systems).

ROIs from experiment 1, we conducted representational similarity analysis between internal processing in experiment 1 (four internal tasks > baseline) and language-related processing in experiment 4 (meaningful sentences > meaningless non-words). This analysis revealed (Fig. 5b and Supplementary Fig. 1c for individual data) the strongest and highly significant similarity (after multiple comparison Bonferroni correction) in the bilateral LTC (left LTC:  $t_{33} = 8.22$ ,  $P < 0.001$ , Cohen's  $d = 1.41$ , 99.375% CI: 0.25 to 0.53; right LTC:  $t_{33} = 9.9$ ,  $P < 0.001$ , Cohen's  $d = 1.7$ , 99.375% CI: 0.29 to 0.53). In addition, a much weaker, but still significant (after multiple comparison Bonferroni correction) similarity was found in the right angular gyrus ( $t_{33} = 3.04$ ,  $P = 0.005$ , Cohen's  $d = 0.52$ , 99.375% CI: 0.01 to 0.39). In the remaining regions, the similarity values were not significant (left PHC:  $t_{33} = 2.58$ ,  $P = 0.014$ , Cohen's  $d = 0.44$ , 99.375% CI:  $-0.01$  to 0.23; left angular gyrus:  $t_{33} = 2.33$ ,  $P = 0.026$ , Cohen's  $d = 0.4$ , 99.375% CI:  $-0.05$  to 0.41; PCC, mPFC and right PHC:  $t_{33} < 1$ ). Examination of direct regional specificity revealed that similarity in the bilateral LTC was significantly higher (after multiple comparison correction) than in the PCC, mPFC and bilateral PHC ( $t_{33} > 5.4$ ,  $P < 0.001$ , Cohen's  $d > 0.93$ ). The right LTC had significantly higher similarity (after multiple comparison correction) compared with the bilateral angular gyrus ( $t_{33} > 3.15$ ,  $P < 0.003$ , Cohen's  $d > 0.54$ ).

The left LTC had significantly higher similarity (after multiple comparison correction) compared with the left angular gyrus ( $t_{33} = 3.15$ ,  $P = 0.003$ , Cohen's  $d = 0.54$ , 99.28% CI: 0.02 to 0.4), but compared with the right angular gyrus the results did not reach significance after multiple comparison ( $t_{33} = 2.68$ ,  $P = 0.01$ , Cohen's  $d = 0.46$ , 99.28% CI:  $-0.01$  to 0.4). Similarity in the right angular gyrus was significantly higher (after multiple comparison correction) only compared with the mPFC ( $t_{33} = 4.05$ ,  $P < 0.001$ , Cohen's  $d = 0.69$ , 99.28% CI: 0.1 to 0.56). Examination of processing type specificity revealed that the bilateral LTC was highly specific relative to both internal processing versus self-referential processing (left LTC:  $t_{31} = 4.55$ ,  $P < 0.001$ , Cohen's  $d = 0.8$ , 99.375% CI: 0.09 to 0.43; right LTC:  $t_{31} = 6.47$ ,  $P < 0.001$ , Cohen's  $d = 1.14$ , 99.375% CI: 0.22 to 0.57) and internal processing versus scene construction (left LTC:  $t_{31} = 7$ ,  $P < 0.001$ , Cohen's  $d = 1.23$ , 99.375% CI: 0.24 to 0.58; right LTC:  $t_{31} = 8.15$ ,  $P < 0.001$ , Cohen's  $d = 1.44$ , 99.375% CI: 0.31 to 0.66).

In addition, we conducted a searchlight representational analysis between internal processing (experiment 1) and scene construction (experiment 4). The unthresholded findings are shown in the top images of Fig. 5c and the significant clusters are shown in the bottom images of Fig. 5c (primary voxel-wise threshold  $P < 0.001$ ; cluster-level threshold  $P < 0.05$ , corrected). In agreement with ROI analysis, the highest similarity was found in the bilateral LTC. The similarity was found to a much lesser extent in the lateral posterior parietal regions, while only the cluster in the right hemisphere reached significance. An additional small cluster was also found in the right superior frontal gyrus (see Supplementary Table 2). We conclude that (1) language-related processing plays a role during internal mentation processing and (2) the bilateral LTC and, to a much lesser extent, the lateral posterior parietal region are the loci of language-related processing during internal mentation.

We also conducted an exploratory representational similarity analysis between individual internal tasks of experiment 1 and experiment 4. We found that similarity during the episodic memory task was lower—particularly in the left LTC—compared with other tasks (see Supplementary Results, 'Representational ROI analysis of individual tasks').

To summarize the key results, significant clusters from the searchlight representational similarity analyses were converted into binary maps. The neural substrates of the three cognitive processes identified are shown in Fig. 6.

## Discussion

In the present study, using four fMRI experiments with the same participants we delineated the neural substrates of three cognitive processes and showed that these neural substrates were active concurrently during self-generated cognition. These findings support the idea that our internal mental experience is the result of a combination of activities from different cognitive (and neural) processes.

The DMN is one of the most explored networks of the human brain<sup>14</sup>. This network specializes in amodal, non-sensory, internally directed cognition and is located at the apex of the processing hierarchy<sup>41,118–120</sup>. According to an influential multi-component account<sup>4</sup>, internal experience is a combination of activity of different cognitive processes operating within the DMN. Through a series of analyses, we identified the neural substrates of three cognitive processes: self-referential processing, mental scene construction and language-related processing (Fig. 6). Our study was designed a priori to focus on these cognitive processes, so our results do not imply that these three processes were the only active processes during internal processing tasks. To specifically delineate cognitive processes during self-generated processing, we used an experimental approach that included separate experiments to elucidate a specific type of processing (that is, experiments 2–4) followed by representational similarity analysis between experiments (see further discussion below). We showed that different cognitive processes all functioned

at the same time during self-generated processing (that is, the internal tasks of experiment 1). Put simply, the participants were lying in a scanner with their eyes closed performing the internal tasks of experiment 1. With the help of experiments 2–4 and especially the use of representational similarity analysis, we established that the mental experience of the participants was a mixture of self-referential, mental scene construction and language-related cognitive processes. We observed that (1) different cognitive processes have specific neural representations, both at the level of regional specificity and processing type specificity and (2) the activity level of the cognitive system could differ across tasks, possibly reflecting the extent to which the process is needed for execution of a specific task (for example, higher activity of the self-referential system while recalling a personal event compared with imagining a non-personal situation; Supplementary Fig. 2a). Our neuroimaging results were paralleled by introspective behavioural reports, showing that participants had vivid scenes in their minds while performing the tasks of experiment 1, but not during the self-referential processing of experiment 2. This suggests that different processes are responsible for different aspects of internal processing. Taken together, our results support the idea that mental experience is mediated by different cognitive processes.

Self-generated cognition in the DMN has been explored extensively, especially over the past decade. Task-based self-generated studies have revealed that while the DMN is involved in processing various self-generated tasks<sup>15,92,121</sup>, the network is also heterogeneous in such a way that different parts of the DMN are selective to specific tasks and types of processing<sup>7,8,18,66–70,122,123</sup>. For example, both autobiographical memory and theory-of-mind tasks activate the frontal and temporal-parietal regions, but the autobiographical memory task activates the midline regions more strongly<sup>7</sup>. The observation that different parts of the DMN are selective to specific tasks supports the multi-component account, but this support is only indirect. First, contrasting between cognitively complex internal tasks (for example, recalling a personal episode versus empathizing with someone), as was done in many previous studies, is unlikely to delineate cognitive processes in a specific way because such tasks are different in many aspects. Second, and even more critical, none of the previous studies (except one; see below) demonstrated several cognitive processes working at the same time. In fact, it does not seem even theoretically possible to show several processes working at the same time when a contrast between two tasks is the analysis method. Another corpus of studies explored spontaneous (that is, non-task-initiated) self-generated cognition in the DMN by correlating across participants' functional<sup>36,75–82</sup> (or anatomical<sup>75</sup>) connectivity during resting scans, with behavioural measures obtained outside the scanner. The researchers found, for example, that specific connectivity patterns in the DMN were associated with behavioural mind-wandering scores<sup>80</sup>, that patterns of hippocampus connectivity were associated with individual autobiographical goals<sup>81</sup> and that connectivity between the PCC and temporal lobe was associated with different features of experience, such as episodic memory and emotions<sup>76</sup>. Overall, the aforementioned resting-state studies revealed the component processes and components of thought, thus supporting the multi-component account. However, given that the functional connectivity measures are based on several minutes of resting scans, and the fact that correlation analyses are conducted across participants, the results of these studies do not directly support the thesis that the specific cognitive experience of an individual person is achieved by several cognitive processes working at the same time. It is noteworthy that some of the previous studies identified components of thought (or types of thought), but not cognitive processes<sup>76–79</sup>. However, it is not evident how components of thought such as 'thinking about the future' or 'being on task' are mapped onto cognitive processes. Overall, while many studies have supported the multi-component account, more direct support is still needed.

To date, the study by Andrews-Hanna et al.<sup>83</sup> has been the only study to provide direct support to the multi-component account, by showing that different cognitive processes work concurrently. A follow-up study by Andrews-Hanna et al.<sup>71</sup> also demonstrated different cognitive processes, but without showing them working together. Compared with the first study by Andrews-Hanna et al.<sup>83</sup>, here we report one largely similar cognitive process (that is, self-related processing), another more specific and restricted cognitive process (that is, current 'mental scene construction' versus previously reported 'mental scene construction and episodic memory') and also an additional cognitive process (language-related processing; see more detailed discussion below). We also extend previous findings by showing that cognitive processes might have variable levels of activity across different tasks (Supplementary Fig. 2). Finally, to identify cognitive processes in the brain, our method does not rely on introspective reports. That is, whereas introspective experience sampling is a valuable tool<sup>5,11,76,77,83</sup>, its general limitation is that participants can report only on matters of which they are aware. For example, in our case, it would have been very difficult—if not impossible—to obtain a reliable report of the extent to which participants used language-related or semantic systems during recall of a past episode from memory. Using our method, it was possible to identify cognitive systems that operate largely unconsciously.

The cognitive systems we identified were mostly confined to the DMN (Fig. 6), corroborating the principal role of the DMN in self-generated cognition. More specifically, self-referential processing was found in the PCC and medial PFC, which is in agreement with the self-referential literature<sup>17,18,20,21,23</sup> and self-related component reported earlier<sup>83</sup>. In addition—again in line with the literature<sup>96</sup>—the self-referential processing system included the lateral parietal cortex region (mostly angular gyrus) with a strong left lateralization (Figs. 3 and 6). The effect of laterality that we found underscores that when the analysis of the DMN is conducted for only one hemisphere (for example, ref.<sup>83</sup>), caution is needed when these results are generalized to another hemisphere. The mental scene-construction cognitive system that we identified exhibited a large locus in the PHC and weaker activity in the retrosplenial and middle occipital cortices (Figs. 4 and 6). These results are in agreement with previous reports, implicating these regions in scene imagery<sup>29</sup> and mental scene construction<sup>25–28</sup>. Some of the brain regions associated with mental scene construction were outside the DMN (Fig. 6). This observation is reminiscent of a recent proposal<sup>103</sup>, according to which the scene-processing system consists of two networks: the first being perceptual-visual (that is, outside the DMN) and the second being non-perceptual, which is related to various types of internal processing (that is, within the DMN). A final note relates to the methodology we used. The use of a perceptual task (that is, visual scenes) as a biomarker to identify mental scene construction was based on a wealth of evidence that there is neural similarity between visual imagery and perception<sup>124–126</sup>. However, despite this similarity, perception and imagery are different phenomena. In particular, the fact that the extent of our scene construction component was relatively limited in the DMN could potentially result from using a perceptual task as a biomarker. In the future, it will be of interest to validate our results using a non-perceptual task as a biomarker to identify mental scene construction processes.

We also successfully delineated language-related processing within the DMN, demonstrating that language-related processing plays a prominent role during internally directed cognition. The loci of language-related activity were very specific, the strongest being in the lateral temporal cortex and, to a much lesser extent, in the lateral posterior parietal cortex (Figs. 5 and 6). These results agree with previous results regarding the role of these regions in semantic processing<sup>33–35</sup>. Notably, our evidence was based on representation analysis, which is a much stronger measure for establishing processing similarities compared with the conjunction analysis (that is, spatial overlap of activations) used previously<sup>33,35</sup>. We found

some level of right lateralization in the lateral posterior parietal cortex (Fig. 5c), although it did not reach significance in a direct test. Interestingly, a very significant opposite (that is, left) lateralization effect was found for self-referential processing (Fig. 3c). Thus, we may observe hemispheric functional specialization at the level of different cognitive processes. It is worth noting that our study did not attempt to elucidate specific types of language-related processing (for example, syntax, inner speech or semantics). In the future, by capitalizing on our approach and methodology, it may be possible to subdivide language-related processing into smaller processes.

An essential aspect of the present work is that we have identified the specific neural substrates of cognitive processes. Delineating specific processes during self-generated processing has traditionally been challenging due to the processes being inherently intertwined. For example, the functional profiles of episodic memory retrieval and self-referential processing<sup>18,86</sup>, episodic and semantic memory<sup>87,88</sup>, as well as episodic memory and mental scene construction<sup>28,84</sup>, are not easily dissociated. To some extent, inaccurate delineation of neural loci of cognitive processes could have potentially contributed to the proposals that there is only one key cognitive process within the DMN<sup>19,27,33,127</sup>. That is, these studies could have attributed a mixture of cognitive processes to a single process. Herein, we ensured specific delineation by selectively manipulating a specific type of processing in experiments 2–4. The neural signature obtained in these experiments was compared with the self-generated internal processing observed in experiment 1. Critically, we found a neural similarity between experiment 1 and experiments 2–4, despite the use of completely different designs, stimuli and tasks, therefore suggesting that we are dealing with a genuine phenomenon. Furthermore, we used representational similarity analysis<sup>97</sup>—an approach that helps establish similarity in information processing<sup>98</sup>. Remarkably, the high similarity we found was in very specific regions and observed through comparison of very specific experiments. This latter observation speaks against the possibility that the correlation reflects some unspecific, cognitively unrelated phenomenon (for example, vascular response). Overall, our experimental approach permitted the achievement of a specific and accurate delineation of cognitive processes. We suggest that our approach can be used in the future to explore additional cognitive systems. In particular, DMN processing in general and specifically the internal tasks used here are to a large extent social in nature<sup>19,43,71,128</sup>. Using our design, we could not estimate and evaluate the role of social processing in the execution of the self-generated tasks of experiment 1. In the future, using the approach proposed here, it should be possible to identify cognitive processes related to social cognition and theory of mind.

In conclusion, the key finding of the present work was that several distinct cognitive processes are active concurrently during internal processing. This result supports the idea that human cognitive experiences may be achieved by pooling over multiple cognitive processes at any given time.

## Methods

**Apparatus.** MRI data were collected using a 3T GE MRI scanner. The key functional MRI echo-planar imaging (EPI) parameters were: repetition time (TR): 2.5 s; echo time (TE): 30 ms; slice thickness: 3.6 mm; in-plane acquisition resolution: 2.08 × 2.08 mm. For more details, see Supplementary Methods.

**Participants.** In total, there were 41 healthy volunteers (mean age: 28, s.d.: 5.07; 17 females; two left-handed). The study was approved by the ethics committee of the Tel Aviv Sourasky Medical Center. Informed written consent was provided by all participants before starting the experiment. Data of five participants were excluded from the analysis due to excessive movements in the scanner (>1 cm). After exclusion of these five participants, the analysis included 36 participants in experiment 1, 34 in experiment 2, 33 in experiment 3 and 34 in experiment 4. Thirty-one participants took part in all experiments. Our sample size was above the current median number of participants in fMRI studies<sup>129</sup> and approximately double the number of participants in key studies in this field<sup>5,26,66,70,95</sup>. In addition to the listed experiments, the study included a

resting-state session (duration: 6 min and 10 s). The resting-state session was not analysed in the present paper.

**Experimental setup.** *Experiment 1: self-generated cognition.* Images of real-life situations were used in the experiment. Participants performed five tasks, defined by an image cue and task instruction (Fig. 1a). Four internal mentation tasks were as follows: (1) past imagery (imagining the situation that had happened before the depicted scene), (2) future imagery (imagining the situation that might happen after the depicted scene), (3) episodic memory (recalling a personal episodic memory event related to the depicted scene) and (4) empathizing (imagining yourself in the place of the person in the image). The baseline condition (rhyme generation) required generation of the words that rhyme with a given word (unrelated to a stimulus image). The structure of the trials is presented in Fig. 1a and was identical for all conditions. All the tasks were executed silently ('in the mind'), without speech. For more details, see Supplementary Methods.

*Experiment 2: self-referential processing.* The material included 54 single Hebrew verbs (infinitive verbs), which can characterize a person (for example, 'to volunteer', 'to smile', 'to lie' or 'to smoke'). The design of these experiments was similar to previous experiments with self-referential tasks<sup>94–96</sup>. The two key conditions of our experiment were: (1) a self-processing condition to decide whether the action described by a verb was characteristic of a participant and (2) a non-self-processing condition to decide whether an action was characteristic of some ideal person. For more details see the Supplementary Methods.

*Experiment 3: visual scenes and objects.* We used a standard visual functional localizer of scene-selective regions<sup>100</sup>, which included images of unfamiliar natural scenes (for example, mountains or lakes) and everyday objects (for example, a ball or a chair). The behavioural task was 'one-back' (that is, to detect the same image that appeared twice in a row). The design was very similar to the one used in our previous study<sup>130</sup>. For more details, see the Supplementary Methods.

*Experiment 4: language-related processing.* The paradigm we used has been shown to reliably localize the language-processing network<sup>105</sup>. The design described below is almost identical to the one used in our previous studies<sup>131,132</sup>. The words (non-words) were presented sequentially at fixation. The two main conditions were written meaningful sentences (comprised of words) and a series of meaningless non-words. Non-words were created as random permutations of the letters, so most of the non-words were unpronounceable and could not be read. The number of letters in the words and non-words was the same. For more details, see Supplementary Methods.

*Behavioural assessment outside the scanner.* After completing all fMRI experiments, participants rated their subjective experiences during scanning on a Likert scale from 1 (low level) to 10 (high level). For establishing the extent to which participants were engaged in self-referential processing during the tasks of experiment 2, we asked them "To what extent was each of the tasks associated with self-related and personal thoughts?". To evaluate mental scene imagery during the execution of tasks in experiments 1 and 2, the participants were asked: "To what extent was each of the tasks associated with having a mental scene in your mind?" Due to technical problems, behavioural reports for three participants are missing.

**Data analysis Preprocessing.** SPM5 (Wellcome Trust Centre for Neuroimaging; <http://www.fil.ion.ucl.ac.uk>) was used for the data analysis. The preprocessing steps included realignment, slice-time correction, motion correction, normalization (2 mm × 2 mm × 3 mm voxel size) and spatial smoothing (full width at half maximum = 6 mm kernel). A unified segmentation procedure<sup>133</sup> was used for normalization. Representational similarity analyses were conducted using non-smoothed data.

*Experiment 1: self-generated cognition.* The data from experiment 1 were split into two parts: the first session and the remaining sessions. The first session was used for defining ROIs (see below) and for illustration of the DMN as a blue contour (Figs. 3–6). The remaining sessions were used for the main analyses. This procedure ensured independent ROI localization<sup>93</sup>.

The first-level fixed effects GLM model (boxcar function) was estimated using five regressors of interest: future imagery, past imagery, episodic memory, empathizing and rhyme generation. Six motion parameters from the preprocessing step were included as the covariate of no interest. The task analysis period was 15 s (task instruction: 4 s; period after instruction: 11 s). A control analysis for only the period after instruction (11 s) yielded qualitatively similar results. For each internal task, we defined first-level contrast as an internal task larger than rhyme generation (four separate contrasts). Four second-level random effects group models were estimated using first-level contrasts. The resulting activation maps were thresholded with a voxel-wise primary threshold  $P < 0.001$  and a cluster-level threshold  $P < 0.05$ , corrected. The primary threshold  $P < 0.001$  has been previously shown to control well for the false positive rate<sup>90,91</sup>. The cluster-level thresholding was done using Monte Carlo simulation using the AlphaSim function in a Resting-State fMRI Data Analysis Toolkit<sup>134</sup>.

This thresholding approach is widely used in the fMRI literature (for example, refs <sup>135–137</sup>). Percent signal change time courses (Fig. 2) were extracted using the MarsBaR region of interest toolbox for SPM<sup>138</sup>.

ROIs were defined individually for each participant as the cluster with the highest DMN selectivity in the first session. ROIs were created automatically (MATLAB custom code<sup>139</sup>) based on the individual DMN peak activations constrained by the parcellation atlas of Craddock et al.<sup>140</sup>. For full details, see Supplementary Methods, 'ROI definition'. The ROI volume was 2,160 mm<sup>3</sup>, which is approximately equivalent to a sphere with a radius of 8 mm. The average location of the ROIs is shown in Fig. 1c and Supplementary Table 1.

Representational similarity analyses<sup>97,141</sup> were performed using spatially non-smoothed data. Here we explain the similarity analysis between experiment 1 (internal processing) and experiment 2 (self-referential processing). Other similarity analyses were conducted using the same logic. In the ROI representational similarity analyses, for each participant and ROI, the first-level analysis contrast values (that is, SPM 'con' images) of experiment 1 (four internal tasks > rhymes generation contrast) and experiment 3 ('self-referential' versus 'non-self-referential') were extracted. Thus, for each region, we obtained two vectors of data (that is, one vector per contrast). We calculated the Spearman's rank correlation between these vectors. Similar results were obtained using Pearson and Kendall tau. Correlation values were subsequently transformed using Fischer r-to-z transform. For each region, transformed correlation values across participants were submitted to a one-sample, two-tailed t-test versus zero. Before this, normality assumptions were validated using the Lilliefors test. Similarity values significantly above zero indicate that there was some degree of similarity between the two types of processing. Bonferroni multiple comparison correction for the number of regions was used (number of regions = 8, alpha = 0.05/8 = 0.00625). To establish regional specificity, we compared similarity values with values of other ROIs. Bonferroni multiple comparison correction for the number of comparisons of each ROI was used (number of comparisons = 7, alpha = 0.05/7 = 0.0071). We also conducted a processing type specificity analysis (see the corresponding section in the Supplementary Methods). In the whole-brain searchlight representational similarity analyses<sup>141,142</sup>, we used a sphere with a radius of 4 mm (268 mm<sup>3</sup>). The results with a larger sphere (radius: 8 mm; volume: 2,145 mm<sup>3</sup>) were generally similar, but a smaller sphere improved spatial specificity. Iteratively, the sphere was moved with a step of one voxel over the whole brain, so that each time a different voxel was used as the centre of a sphere<sup>143</sup>. At the end of the process, the similarity values for each voxel were averaged<sup>143</sup>. Significance was established at the group level (that is, across subjects) using a one-sample, two-tailed t-test versus zero. The resulting activation maps were thresholded using exactly the same procedure used in the GLM analysis: a voxel-wise primary threshold  $P < 0.001$  and a cluster-level threshold  $P < 0.05$ , corrected (cluster size was established using Monte Carlo simulation<sup>134</sup>). The unthresholded statistical maps were also shown (Figs. 3c, 4c and 5c).

**Experiment 2: self-referential processing.** The first-level GLM model (boxcar function) was estimated for each participant using three regressors of interest (that is, self-processing, non-self-processing and letters comparison) and six motion parameters as regressors of no interest. To assess self-referential selectivity, the SPM contrast 'self-processing > non-self-processing' was used.

**Experiment 3: visual scenes and objects.** The first-level GLM model (boxcar function) was estimated for each participant using two regressors of interest (scenes and objects conditions) and six motion parameters as regressors of no interest.

**Experiment 4: language-related processing.** The first-level GLM model (boxcar function) was estimated for each participant using two regressors of interest (meaningful sentences and non-words) and six motion parameters as regressors of no interest.

**Life Sciences Reporting Summary.** Further information on experimental design is available in the Life Sciences Reporting Summary.

**Code availability.** The custom code used in this study is available from the corresponding author upon reasonable request.

**Data availability.** The data supporting the findings of this study are available from the corresponding author upon reasonable request.

Received: 19 September 2016; Accepted: 17 October 2017;  
Published online: 4 December 2017

## References

- Smallwood, J. & Schooler, J. W. The science of mind wandering: empirically navigating the stream of consciousness. *Annu. Rev. Psychol.* **66**, 487–518 (2015).
- Killingsworth, M. A. & Gilbert, D. T. A wandering mind is an unhappy mind. *Science* **330**, 932 (2010).
- Smallwood, J. Distinguishing how from why the mind wanders: a process–occurrence framework for self-generated mental activity. *Psychol. Bull.* **139**, 519–535 (2013).
- Andrews-Hanna, J. R., Smallwood, J. & Spreng, R. N. The default network and self-generated thought: component processes, dynamic control, and clinical relevance. *Ann. NY Acad. Sci.* **1316**, 29–52 (2014).
- Addis, D. R., Wong, A. T. & Schacter, D. L. Remembering the past and imagining the future: common and distinct neural substrates during event construction and elaboration. *Neuropsychologia* **45**, 1363–1377 (2007).
- Addis, D. R., Pan, L., Vu, M.-A., Laiser, N. & Schacter, D. L. Constructive episodic simulation of the future and the past: distinct subsystems of a core brain network mediate imagining and remembering. *Neuropsychologia* **47**, 2222–2238 (2009).
- Rabin, J. S., Gilboa, A., Stuss, D. T., Mar, R. A. & Rosenbaum, R. S. Common and unique neural correlates of autobiographical memory and theory of mind. *J. Cogn. Neurosci.* **22**, 1095–1111 (2010).
- Rabin, J. S. & Rosenbaum, R. S. Familiarity modulates the functional relationship between theory of mind and autobiographical memory. *Neuroimage* **62**, 520–529 (2012).
- Axelrod, V., Rees, G., Lavidor, M. & Bar, M. Increasing propensity to mind wander with transcranial direct current stimulation. *Proc. Natl Acad. Sci. USA* **112**, 3314–3319 (2015).
- Christoff, K., Gordon, A. M., Smallwood, J., Smith, R. & Schooler, J. W. Experience sampling during fMRI reveals default network and executive system contributions to mind wandering. *Proc. Natl Acad. Sci. USA* **106**, 8719–8724 (2009).
- Stawarczyk, D., Majerus, S., Maquet, P. & D'Argembeau, A. Neural correlates of ongoing conscious experience: both task-unrelatedness and stimulus-independence are related to default network activity. *PLoS ONE* **6**, e16997 (2011).
- Smallwood, J. & Schooler, J. W. The restless mind. *Psychol. Bull.* **132**, 946–958 (2006).
- Buckner, R. L., Andrews-Hanna, J. R. & Schacter, D. L. The brain's default network: anatomy, function, and relevance to disease. *Ann. NY Acad. Sci.* **1124**, 1–38 (2008).
- Raichle, M. E. The brain's default mode network. *Annu. Rev. Neurosci.* **38**, 433–447 (2015).
- Stawarczyk, D. & D'Argembeau, A. Neural correlates of personal goal processing during episodic future thinking and mind-wandering: an ALE meta-analysis. *Hum. Brain Mapp.* **36**, 2928–2947 (2015).
- Fox, K. C., Spreng, R. N., Ellamil, M., Andrews-Hanna, J. R. & Christoff, K. The wandering brain: meta-analysis of functional neuroimaging studies of mind-wandering and related spontaneous thought processes. *Neuroimage* **111**, 611–621 (2015).
- Northoff, G. et al. Self-referential processing in our brain—a meta-analysis of imaging studies on the self. *Neuroimage* **31**, 440–457 (2006).
- Sajonz, B. et al. Delineating self-referential processing from episodic memory retrieval: common and dissociable networks. *Neuroimage* **50**, 1606–1617 (2010).
- Buckner, R. L. & Carroll, D. C. Self-projection and the brain. *Trends Cogn. Sci.* **11**, 49–57 (2007).
- Qin, P. & Northoff, G. How is our self related to midline regions and the default-mode network? *Neuroimage* **57**, 1221–1233 (2011).
- Whitfield-Gabrieli, S. et al. Associations and dissociations between default and self-reference networks in the human brain. *Neuroimage* **55**, 225–232 (2011).
- Kurczek, J. et al. Differential contributions of hippocampus and medial prefrontal cortex to self-projection and self-referential processing. *Neuropsychologia* **73**, 116–126 (2015).
- Moran, J. M., Kelley, W. M. & Heatherton, T. F. What can the organization of the brain's default mode network tell us about self-knowledge? *Front. Hum. Neurosci.* **7**, 391 (2013).
- Kim, H. A dual-subsystem model of the brain's default network: self-referential processing, memory retrieval processes, and autobiographical memory retrieval. *NeuroImage* **61**, 966–977 (2012).
- Palombo, D., Hayes, S., Peterson, K., Keane, M. & Verfaellie, M. Medial temporal lobe contributions to episodic future thinking: scene construction or future projection? *Cereb. Cortex* <https://doi.org/10.1093/cercor/bhw381> (2016).
- Hassabis, D., Kumaran, D. & Maguire, E. A. Using imagination to understand the neural basis of episodic memory. *J. Neurosci.* **27**, 14365–14374 (2007).
- Hassabis, D. & Maguire, E. A. Deconstructing episodic memory with construction. *Trends Cogn. Sci.* **11**, 299–306 (2007).
- Hassabis, D., Kumaran, D., Vann, S. D. & Maguire, E. A. Patients with hippocampal amnesia cannot imagine new experiences. *Proc. Natl Acad. Sci. USA* **104**, 1726–1731 (2007).
- Bird, C. M., Capponi, C., King, J. A., Doeller, C. F. & Burgess, N. Establishing the boundaries: the hippocampal contribution to imagining scenes. *J. Neurosci.* **30**, 11688–11695 (2010).

30. Nyberg, L., Kim, A. S., Habib, R., Levine, B. & Tulving, E. Consciousness of subjective time in the brain. *Proc. Natl Acad. Sci. USA* **107**, 22356–22359 (2010).
31. Tulving, E. in *Principles of Frontal Lobe Function* (eds Stuss, D. T. & Knight, R. C.) Ch. 20 (Oxford Univ. Press, New York, NY, 2002).
32. Peer, M., Salomon, R., Goldberg, I., Blanke, O. & Arzy, S. Brain system for mental orientation in space, time, and person. *Proc. Natl Acad. Sci. USA* **112**, 11072–11077 (2015).
33. Binder, J. R., Desai, R. H., Graves, W. W. & Conant, L. L. Where is the semantic system? A critical review and meta-analysis of 120 functional neuroimaging studies. *Cereb. Cortex* **19**, 2767–2796 (2009).
34. Davey, J. et al. Automatic and controlled semantic retrieval: TMS reveals distinct contributions of posterior middle temporal gyrus and angular gyrus. *J. Neurosci.* **35**, 15230–15239 (2015).
35. Humphreys, G. F., Hoffman, P., Visser, M., Binney, R. J. & Ralph, M. A. L. Establishing task- and modality-dependent dissociations between the semantic and default mode networks. *Proc. Natl Acad. Sci. USA* **112**, 7857–7862 (2015).
36. Vatansever, D. et al. Varieties of semantic cognition revealed through simultaneous decomposition of intrinsic brain connectivity and behaviour. *Neuroimage* **158**, 1–11 (2017).
37. Sestieri, C., Corbetta, M., Romani, G. L. & Shulman, G. L. Episodic memory retrieval, parietal cortex, and the default mode network: functional and topographic analyses. *J. Neurosci.* **31**, 4407–4420 (2011).
38. Sestieri, C., Shulman, G. L. & Corbetta, M. The contribution of the human posterior parietal cortex to episodic memory. *Nat. Rev. Neurosci.* **18**, 183–192 (2017).
39. Rugg, M. D. & Vilberg, K. L. Brain networks underlying episodic memory retrieval. *Curr. Opin. Neurobiol.* **23**, 255–260 (2013).
40. Foster, B. L., Rangarajan, V., Shirer, W. R. & Parvizi, J. Intrinsic and task-dependent coupling of neuronal population activity in human parietal cortex. *Neuron* **86**, 578–590 (2015).
41. Chen, J. et al. Shared memories reveal shared structure in neural activity across individuals. *Nat. Neurosci.* **20**, 115–125 (2017).
42. Hirshhorn, M., Grady, C., Rosenbaum, R. S., Winocur, G. & Moscovitch, M. Brain regions involved in the retrieval of spatial and episodic details associated with a familiar environment: an fMRI study. *Neuropsychologia* **50**, 3094–3106 (2012).
43. Mars, R. B. et al. On the relationship between the “default mode network” and the “social brain”. *Front. Hum. Neurosci.* **6**, 189 (2012).
44. Spreng, R. & Andrews-Hanna, J. in *Brain Mapping: An Encyclopedic Reference* (ed. Toga, A. W.) 165–169 (Academic Press, Cambridge, MA, 2015).
45. Schilbach, L., Eickhoff, S. B., Rotarska-Jagiela, A., Fink, G. R. & Vogeley, K. Minds at rest? Social cognition as the default mode of cognizing and its putative relationship to the “default system” of the brain. *Conscious. Cogn.* **17**, 457–467 (2008).
46. Mitchell, J. P., Banaji, M. R. & Macrae, C. N. The link between social cognition and self-referential thought in the medial prefrontal cortex. *J. Cogn. Neurosci.* **17**, 1306–1315 (2005).
47. Gilead, M. et al. Self-regulation via neural simulation. *Proc. Natl Acad. Sci. USA* **113**, 10037–10042 (2016).
48. Hill, P. E., Yi, R., Spreng, R. N. & Diana, R. A. Neural congruence between intertemporal and interpersonal self-control: evidence from delay and social discounting. *Neuroimage* **162**, 186–198 (2017).
49. Saxe, R. & Kanwisher, N. People thinking about thinking people: the role of the temporo-parietal junction in “theory of mind”. *Neuroimage* **19**, 1835–1842 (2003).
50. Tusche, A., Smallwood, J., Bernhardt, B. C. & Singer, T. Classifying the wandering mind: revealing the affective content of thoughts during task-free rest periods. *Neuroimage* **97**, 107–116 (2014).
51. Maysless, N., Eran, A. & Shamay-Tsoory, S. G. Generating original ideas: the neural underpinning of originality. *Neuroimage* **116**, 232–239 (2015).
52. Beaty, R. E. et al. Creativity and the default network: a functional connectivity analysis of the creative brain at rest. *Neuropsychologia* **64**, 92–98 (2014).
53. Laird, A. R. et al. Investigating the functional heterogeneity of the default mode network using coordinate-based meta-analytic modeling. *J. Neurosci.* **29**, 14496–14505 (2009).
54. Leech, R., Braga, R. & Sharp, D. J. Echoes of the brain within the posterior cingulate cortex. *J. Neurosci.* **32**, 215–222 (2012).
55. Mars, R. B. et al. Connectivity-based subdivisions of the human right “temporoparietal junction area”: evidence for different areas participating in different cortical networks. *Cereb. Cortex* **22**, 1894–1903 (2012).
56. Bzdok, D. et al. Subspecialization in the human posterior medial cortex. *Neuroimage* **106**, 55–71 (2015).
57. Bzdok, D. et al. Characterization of the temporo-parietal junction by combining data-driven parcellation, complementary connectivity analyses, and functional decoding. *Neuroimage* **81**, 381–392 (2013).
58. Leech, R., Kamourieh, S., Beckmann, C. F. & Sharp, D. J. Fractionating the default mode network: distinct contributions of the ventral and dorsal posterior cingulate cortex to cognitive control. *J. Neurosci.* **31**, 3217–3224 (2011).
59. Dastjerdi, M. et al. Differential electrophysiological response during rest, self-referential, and non-self-referential tasks in human posteromedial cortex. *Proc. Natl Acad. Sci. USA* **108**, 3023–3028 (2011).
60. Seghier, M. L., Fagan, E. & Price, C. J. Functional subdivisions in the left angular gyrus where the semantic system meets and diverges from the default network. *J. Neurosci.* **30**, 16809–16817 (2010).
61. Braga, R. M. & Buckner, R. L. Parallel interdigitated distributed networks within the individual estimated by intrinsic functional connectivity. *Neuron* **95**, 457–471.e5 (2017).
62. Braga, R. M., Sharp, D. J., Leeson, C., Wise, R. J. & Leech, R. Echoes of the brain within default mode, association, and heteromodal cortices. *J. Neurosci.* **33**, 14031–14039 (2013).
63. Utevsky, A. V., Smith, D. V. & Huettel, S. A. Precuneus is a functional core of the default-mode network. *J. Neurosci.* **34**, 932–940 (2014).
64. Ramot, M. et al. A widely distributed spectral signature of task-negative electrocorticography responses revealed during a visumotor task in the human cortex. *J. Neurosci.* **32**, 10458–10469 (2012).
65. Bellana, B., Liu, Z. X., Diamond, N., Grady, C. & Moscovitch, M. Similarities and differences in the default mode network across rest, retrieval, and future imagining. *Hum. Brain Mapp.* **38**, 1155–1171 (2017).
66. Spreng, R. N. & Grady, C. L. Patterns of brain activity supporting autobiographical memory, prospection, and theory of mind, and their relationship to the default mode network. *J. Cogn. Neurosci.* **22**, 1112–1123 (2009).
67. D’Argebeau, A. et al. The neural basis of personal goal processing when envisioning future events. *J. Cogn. Neurosci.* **22**, 1701–1713 (2010).
68. Tamir, D. I., Bricker, A. B., Dodell-Feder, D. & Mitchell, J. P. Reading fiction and reading minds: the role of simulation in the default network. *Soc. Cogn. Affect. Neurosci.* **11**, 215–224 (2015).
69. Abraham, A., Schubotz, R. I. & von Cramon, D. Y. Thinking about the future versus the past in personal and non-personal contexts. *Brain Res.* **1233**, 106–119 (2008).
70. Szpunar, K. K., Watson, J. M. & McDermott, K. B. Neural substrates of envisioning the future. *Proc. Natl Acad. Sci. USA* **104**, 642–647 (2007).
71. Andrews-Hanna, J. R., Saxe, R. & Yarkoni, T. Contributions of episodic retrieval and mentalizing to autobiographical thought: evidence from functional neuroimaging, resting-state connectivity, and fMRI meta-analyses. *Neuroimage* **91**, 324–335 (2014).
72. Preminger, S., Harmelech, T. & Malach, R. Stimulus-free thoughts induce differential activation in the human default network. *Neuroimage* **54**, 1692–1702 (2011).
73. Harrison, B. J. et al. Consistency and functional specialization in the default mode brain network. *Proc. Natl Acad. Sci. USA* **105**, 9781–9786 (2008).
74. Shapira-Lichter, I., Oren, N., Jacob, Y., Gruberger, M. & Hendler, T. Portraying the unique contribution of the default mode network to internally driven mnemonic processes. *Proc. Natl Acad. Sci. USA* **110**, 4950–4955 (2013).
75. Karapanagiotidis, T., Bernhardt, B. C., Jefferies, E. & Smallwood, J. Tracking thoughts: exploring the neural architecture of mental time travel during mind-wandering. *Neuroimage* **147**, 272–281 (2017).
76. Smallwood, J. et al. Representing representation: integration between the temporal lobe and the posterior cingulate influences the content and form of spontaneous thought. *PLoS ONE* **11**, e0152272 (2016).
77. Gorgolewski, K. J. et al. A correspondence between individual differences in the brain’s intrinsic functional architecture and the content and form of self-generated thoughts. *PLoS ONE* **9**, e97176 (2014).
78. Andrews-Hanna, J. R., Reidler, J. S., Huang, C. & Buckner, R. L. Evidence for the default network’s role in spontaneous cognition. *J. Neurophysiol.* **104**, 322–335 (2010).
79. Doucet, G. et al. Patterns of hemodynamic low-frequency oscillations in the brain are modulated by the nature of free thought during rest. *Neuroimage* **59**, 3194–3200 (2012).
80. Poerio, G. L. et al. The role of the default mode network in component processes underlying the wandering mind. *Soc. Cogn. Affect. Neurosci.* **12**, 1047–1062 (2017).
81. Medea, B. et al. How do we decide what to do? Resting-state connectivity patterns and components of self-generated thought linked to the development of more concrete personal goals. *Exp. Brain Res.* <https://doi.org/10.1007/s00221-016-4729-y> (2016).
82. De Caso, I., Poerio, G., Jefferies, E. & Smallwood, J. That’s me in the spotlight: neural basis of individual differences in self-consciousness. *Soc. Cogn. Affect. Neurosci.* **12**, 1384–1393 (2017).
83. Andrews-Hanna, J. R., Reidler, J. S., Sepulcre, J., Poulin, R. & Buckner, R. L. Functional-anatomic fractionation of the brain’s default network. *Neuron* **65**, 550–562 (2010).

84. Kim, S., Dede, A. J., Hopkins, R. O. & Squire, L. R. Memory, scene construction, and the human hippocampus. *Proc. Natl Acad. Sci. USA* **112**, 4767–4772 (2015).
85. Xu, X., Yuan, H. & Lei, X. Activation and connectivity within the default mode network contribute independently to future-oriented thought. *Sci. Rep.* **6**, 21001 (2016).
86. Summerfield, J. J., Hassabis, D. & Maguire, E. A. Cortical midline involvement in autobiographical memory. *Neuroimage* **44**, 1188–1200 (2009).
87. Irish, M. & Piguet, O. The pivotal role of semantic memory in remembering the past and imagining the future. *Front. Behav. Neurosci.* **7**, 27 (2013).
88. Kim, H. Default network activation during episodic and semantic memory retrieval: a selective meta-analytic comparison. *Neuropsychologia* **80**, 35–46 (2016).
89. Burianova, H. & Grady, C. L. Common and unique neural activations in autobiographical, episodic, and semantic retrieval. *J. Cogn. Neurosci.* **19**, 1520–1534 (2007).
90. Woo, C.-W., Krishnan, A. & Wager, T. D. Cluster-extent based thresholding in fMRI analyses: pitfalls and recommendations. *Neuroimage* **91**, 412–419 (2014).
91. Eklund, A., Nichols, T. E. & Knutsson, H. Cluster failure: why fMRI inferences for spatial extent have inflated false-positive rates. *Proc. Natl Acad. Sci. USA* **113**, 7900–7905 (2016).
92. Spreng, R. N., Mar, R. A. & Kim, A. S. N. The common neural basis of autobiographical memory, prospection, navigation, theory of mind, and the default mode: a quantitative meta-analysis. *J. Cogn. Neurosci.* **21**, 489–510 (2008).
93. Kriegeskorte, N., Simmons, W. K., Bellgowan, P. S. F. & Baker, C. I. Circular analysis in systems neuroscience: the dangers of double dipping. *Nat. Neurosci.* **12**, 535–540 (2009).
94. Kelley, W. M. et al. Finding the self? An event-related fMRI study. *J. Cogn. Neurosci.* **14**, 785–794 (2002).
95. Goldberg, I. I., Harel, M. & Malach, R. When the brain loses its self: prefrontal inactivation during sensorimotor processing. *Neuron* **50**, 329–339 (2006).
96. Murray, R. J., Schaer, M. & Debbané, M. Degrees of separation: a quantitative neuroimaging meta-analysis investigating self-specificity and shared neural activation between self- and other-reflection. *Neurosci. Biobehav. Rev.* **36**, 1043–1059 (2012).
97. Kriegeskorte, N. & Kievit, R. A. Representational geometry: integrating cognition, computation, and the brain. *Trends Cogn. Sci.* **17**, 401–412 (2013).
98. Raizada, R. D. S. & Kriegeskorte, N. Pattern-information fMRI: new questions which it opens up and challenges which face it. *Int. J. Imag. Syst. Technol.* **20**, 31–41 (2010).
99. Oosterhof, N. N., Wiggett, A. J., Diedrichsen, J., Tipper, S. P. & Downing, P. E. Surface-based information mapping reveals crossmodal vision–action representations in human parietal and occipitotemporal cortex. *J. Neurophysiol.* **104**, 1077–1089 (2010).
100. Aminoff, E. M., Kveraga, K. & Bar, M. The role of the parahippocampal cortex in cognition. *Trends Cogn. Sci.* **17**, 379–390 (2013).
101. Epstein, R. & Kanwisher, N. A cortical representation of the local visual environment. *Nature* **392**, 598–601 (1998).
102. Epstein, R. A. Parahippocampal and retrosplenial contributions to human spatial navigation. *Trends Cogn. Sci.* **12**, 388–396 (2008).
103. Baldassano, C., Esteva, A., Fei-Fei, L. & Beck, D. M. Two distinct scene-processing networks connecting vision and memory. *eNeuro* **3**, 0178–16.2016 (2016).
104. Price, C. J. A review and synthesis of the first 20 years of PET and fMRI studies of heard speech, spoken language and reading. *Neuroimage* **62**, 816–847 (2012).
105. Fedorenko, E., Hsieh, P.-J., Nieto-Castañón, A., Whitfield-Gabrieli, S. & Kanwisher, N. New method for fMRI investigations of language: defining ROIs functionally in individual subjects. *J. Neurophysiol.* **104**, 1177–1194 (2010).
106. Vigneau, M. et al. Meta-analyzing left hemisphere language areas: phonology, semantics, and sentence processing. *Neuroimage* **30**, 1414–1432 (2006).
107. Fedorenko, E. & Thompson-Schill, S. L. Reworking the language network. *Trends Cogn. Sci.* **18**, 120–126 (2014).
108. Friederici, A. D. The brain basis of language processing: from structure to function. *Physiol. Rev.* **91**, 1357–1392 (2011).
109. Seghier, M. L. The angular gyrus multiple functions and multiple subdivisions. *Neuroscientist* **19**, 43–61 (2013).
110. Simony, E. et al. Dynamic reconfiguration of the default mode network during narrative comprehension. *Nat. Commun.* **7**, 12141 (2016).
111. Bookheimer, S. Functional MRI of language: new approaches to understanding the cortical organization of semantic processing. *Annu. Rev. Neurosci.* **25**, 151–188 (2002).
112. Patterson, K., Nestor, P. J. & Rogers, T. T. Where do you know what you know? The representation of semantic knowledge in the human brain. *Nat. Rev. Neurosci.* **8**, 976–987 (2007).
113. Ross, L. A. & Olson, I. R. What's unique about unique entities? An fMRI investigation of the semantics of famous faces and landmarks. *Cereb. Cortex* **22**, 2005–2015 (2011).
114. Axelrod, V. & Yovel, G. Successful decoding of famous faces in the fusiform face area. *PLoS ONE* **10**, e0117126 (2015).
115. Wirth, M. et al. Semantic memory involvement in the default mode network: a functional neuroimaging study using independent component analysis. *Neuroimage* **54**, 3057–3066 (2011).
116. Jackson, R. L., Hoffman, P., Pobric, G. & Ralph, M. A. L. The semantic network at work and rest: differential connectivity of anterior temporal lobe subregions. *J. Neurosci.* **36**, 1490–1501 (2016).
117. Krieger-Redwood, K. et al. Down but not out in posterior cingulate cortex: deactivation yet functional coupling with prefrontal cortex during demanding semantic cognition. *Neuroimage* **141**, 366–377 (2016).
118. Margulies, D. S. et al. Situating the default-mode network along a principal gradient of macroscale cortical organization. *Proc. Natl Acad. Sci. USA* **113**, 12574–12579 (2016).
119. Hasson, U., Chen, J. & Honey, C. J. Hierarchical process memory: memory as an integral component of information processing. *Trends Cogn. Sci.* **19**, 304–313 (2015).
120. Golland, Y. et al. Extrinsic and intrinsic systems in the posterior cortex of the human brain revealed during natural sensory stimulation. *Cereb. Cortex* **17**, 766–777 (2007).
121. Benoit, R. G. & Schacter, D. L. Specifying the core network supporting episodic simulation and episodic memory by activation likelihood estimation. *Neuropsychologia* **75**, 450–457 (2015).
122. Grady, C. L. et al. A multivariate analysis of age-related differences in default mode and task-positive networks across multiple cognitive domains. *Cereb. Cortex* **20**, 1432–1447 (2009).
123. Salomon, R., Levy, D. R. & Malach, R. Deconstructing the default: cortical subdivision of the default mode/intrinsic system during self-related processing. *Hum. Brain Mapp.* **35**, 1491–1502 (2013).
124. O'Craven, K. M. & Kanwisher, N. Mental imagery of faces and places activates corresponding stimulus-specific brain regions. *J. Cogn. Neurosci.* **12**, 1013–1023 (2000).
125. Cichy, R. M., Heinze, J. & Haynes, J.-D. Imagery and perception share cortical representations of content and location. *Cereb. Cortex* **22**, 372–380 (2012).
126. Reddy, L., Tsuchiya, N. & Serre, T. Reading the mind's eye: decoding category information during mental imagery. *Neuroimage* **50**, 818–825 (2010).
127. Bar, M., Aminoff, E., Mason, M. & Fenske, M. The units of thought. *Hippocampus* **17**, 420–428 (2007).
128. Chavez, R. S. & Heatherton, T. F. Representational similarity of social and valence information in the medial pFC. *J. Cogn. Neurosci.* **27**, 73–82 (2015).
129. Poldrack, R. A. et al. Scanning the horizon: towards transparent and reproducible neuroimaging research. *Nat. Rev. Neurosci.* **18**, 115–126 (2017).
130. Axelrod, V. & Yovel, G. Hierarchical processing of face viewpoint in human visual cortex. *J. Neurosci.* **32**, 2442–2452 (2012).
131. Axelrod, V., Bar, M., Rees, G. & Yovel, G. Neural correlates of subliminal language processing. *Cereb. Cortex* **25**, 2160–2169 (2015).
132. Axelrod, V. On the domain-specificity of the visual and non-visual face-selective regions. *Eur. J. Neurosci.* **44**, 2049–2063 (2016).
133. Ashburner, J. & Friston, K. J. Unified segmentation. *Neuroimage* **26**, 839–851 (2005).
134. Song, X.-W. et al. REST: a toolkit for resting-state functional magnetic resonance imaging data processing. *PLoS ONE* **6**, e25031 (2011).
135. Siuda-Krzywicka, K. et al. Massive cortical reorganization in sighted Braille readers. *eLife* **5**, e10762 (2016).
136. Wang, L. et al. Changes in hippocampal connectivity in the early stages of Alzheimer's disease: evidence from resting state fMRI. *Neuroimage* **31**, 496–504 (2006).
137. Zald, D. H. et al. Midbrain dopamine receptor availability is inversely associated with novelty-seeking traits in humans. *J. Neurosci.* **28**, 14372–14378 (2008).
138. Brett, M., Anton, J., Valabregue, R. & Poline, J. Region of interest analysis using an SPM toolbox. *Neuroimage* **16**, 497 (2002).
139. Axelrod, V. Minimizing bugs in cognitive neuroscience programming. *Front. Psychol.* **5**, 1435 (2014).
140. Craddock, R. C., James, G. A., Holtzheimer, P. E., Hu, X. P. & Mayberg, H. S. A whole brain fMRI atlas generated via spatially constrained spectral clustering. *Hum. Brain Mapp.* **33**, 1914–1928 (2012).
141. Nili, H. et al. A toolbox for representational similarity analysis. *PLoS Comput. Biol.* **10**, e1003553 (2014).
142. Etzel, J. A., Zacks, J. M. & Braver, T. S. Searchlight analysis: promise, pitfalls, and potential. *Neuroimage* **78**, 261–269 (2013).
143. Björnsdóttir, M., Rylander, K. & Wessberg, J. A Monte Carlo method for locally multivariate brain mapping. *Neuroimage* **56**, 508–516 (2011).

### Acknowledgements

This work was supported by the Yad Hanadiv Rothschild fellowship (to V.A.), the Wellcome Trust (to G.R.) and the Israeli Center of Research Excellence in Cognitive Sciences (to M.B.). We also thank K. Siuda-Krzywicka and S. Schwarzkopf for advice, and N. Hale for technical assistance. No funders had any role in study design, data collection and analysis, decision to publish or preparation of the manuscript.

### Author contributions

V.A. and M.B. conceived the study. V.A. designed and performed the study. V.A. analysed the data with input from G.R. and M.B. V.A., G.R. and M.B. wrote the paper.

### Competing interests

The authors declare no competing interests.

### Additional information

**Supplementary information** is available for this paper at <https://doi.org/10.1038/s41562-017-0244-9>.

**Reprints and permissions information** is available at [www.nature.com/reprints](http://www.nature.com/reprints).

**Correspondence and requests for materials** should be addressed to V.A.

**Publisher's note:** Springer Nature remains neutral with regard to jurisdictional claims in published maps and institutional affiliations.

## Life Sciences Reporting Summary

Nature Research wishes to improve the reproducibility of the work that we publish. This form is intended for publication with all accepted life science papers and provides structure for consistency and transparency in reporting. Every life science submission will use this form; some list items might not apply to an individual manuscript, but all fields must be completed for clarity.

For further information on the points included in this form, see [Reporting Life Sciences Research](#). For further information on Nature Research policies, including our [data availability policy](#), see [Authors & Referees](#) and the [Editorial Policy Checklist](#).

### ▶ Experimental design

#### 1. Sample size

Describe how sample size was determined.

Our sample size was above the current median number of participants in fMRI studies (Poldrack et al., 2017) and approximately double the number of participants in key studies in this field (Goldberg et al., 2006; Addis et al., 2007; Hassabis et al., 2007; Szpunar et al., 2007; Spreng and Grady, 2009).

#### 2. Data exclusions

Describe any data exclusions.

Data of five participants were excluded from the analysis due to excessive movements in the scanner (>1 cm).

#### 3. Replication

Describe whether the experimental findings were reliably reproduced.

Our findings are in line with large number of previous studies. We show individual data that demonstrate consistency of our findings.

#### 4. Randomization

Describe how samples/organisms/participants were allocated into experimental groups.

N/A (there were no experimental groups)

#### 5. Blinding

Describe whether the investigators were blinded to group allocation during data collection and/or analysis.

N/A (there were no experimental groups)

Note: all studies involving animals and/or human research participants must disclose whether blinding and randomization were used.

#### 6. Statistical parameters

For all figures and tables that use statistical methods, confirm that the following items are present in relevant figure legends (or in the Methods section if additional space is needed).

- |                                     |  |
|-------------------------------------|--|
| n/a                                 | Confirmed  |
| <input type="checkbox"/>            | <input checked="" type="checkbox"/> The <u>exact sample size</u> ( <i>n</i> ) for each experimental group/condition, given as a discrete number and unit of measurement (animals, litters, cultures, etc.)                               |
| <input type="checkbox"/>            | <input checked="" type="checkbox"/> A description of how samples were collected, noting whether measurements were taken from distinct samples or whether the same sample was measured repeatedly   |
| <input checked="" type="checkbox"/> | <input type="checkbox"/> A statement indicating how many times each experiment was replicated  |
| <input type="checkbox"/>            | <input checked="" type="checkbox"/> The statistical test(s) used and whether they are one- or two-sided (note: only common tests should be described solely by name; more complex techniques should be described in the Methods section) |
| <input type="checkbox"/>            | <input checked="" type="checkbox"/> A description of any assumptions or corrections, such as an adjustment for multiple comparisons  |
| <input type="checkbox"/>            | <input checked="" type="checkbox"/> The test results (e.g. <i>P</i> values) given as exact values whenever possible and with confidence intervals noted  |
| <input type="checkbox"/>            | <input checked="" type="checkbox"/> A clear description of statistics including <u>central tendency</u> (e.g. median, mean) and <u>variation</u> (e.g. standard deviation, interquartile range)  |
| <input type="checkbox"/>            | <input checked="" type="checkbox"/> Clearly defined error bars   |

See the web collection on [statistics for biologists](#) for further resources and guidance.

## ► Software

Policy information about [availability of computer code](#)

### 7. Software

Describe the software used to analyze the data in this study.

SPM5 (Wellcome Trust Centre for Neuroimaging, London, UK; <http://www.fil.ion.ucl.ac.uk>), MATLAB R2009B

For manuscripts utilizing custom algorithms or software that are central to the paper but not yet described in the published literature, software must be made available to editors and reviewers upon request. We strongly encourage code deposition in a community repository (e.g. GitHub). *Nature Methods* [guidance for providing algorithms and software for publication](#) provides further information on this topic.

## ► Materials and reagents

Policy information about [availability of materials](#)

### 8. Materials availability

Indicate whether there are restrictions on availability of unique materials or if these materials are only available for distribution by a for-profit company.

N/A

### 9. Antibodies

Describe the antibodies used and how they were validated for use in the system under study (i.e. assay and species).

N/A

### 10. Eukaryotic cell lines

a. State the source of each eukaryotic cell line used.

N/A

b. Describe the method of cell line authentication used.

N/A

c. Report whether the cell lines were tested for mycoplasma contamination.

N/A

d. If any of the cell lines used are listed in the database of commonly misidentified cell lines maintained by [ICLAC](#), provide a scientific rationale for their use.

N/A

## ► Animals and human research participants

Policy information about [studies involving animals](#); when reporting animal research, follow the [ARRIVE guidelines](#)

### 11. Description of research animals

Provide details on animals and/or animal-derived materials used in the study.

no animal were used

Policy information about [studies involving human research participants](#)

### 12. Description of human research participants

Describe the covariate-relevant population characteristics of the human research participants.

Forty-one healthy volunteers: average age: 28 (standard deviation: 5.07), 17 females, two left-handed.

## MRI Studies Reporting Summary

Form fields will expand as needed. Please do not leave fields blank.

### ▶ Experimental design

1. Describe the experimental design.

All four experiments used block design.

Experiment 1: five conditions ("future imagery", "past imagery", "episodic memory", "empathizing", and "rhyme generation").

Experiment 2: three conditions ("self-processing", "non-self-processing" and "letters comparison"). The "letters comparison" condition was not analyzed here.

Experiment 3: three conditions ("scenes", "objects" and "faces"). The "faces" condition was not analyzed here.

Experiment 4: two conditions ("sentences" and "non-words").

2. Specify the number of blocks, trials or experimental units per session and/or subject, and specify the length of each trial or block (if trials are blocked) and interval between trials.

Experiment 1: Block duration: 25 sec. Interval between blocks: 1 sec. A scanning session included 15 trials, with 3 trials per condition. 15 trials per session. Thirty-two participants completed five experimental sessions and four participants completed four sessions.

Experiment 2: Block duration: 25 seconds. Interval between blocks: 2.5 sec. Two types of sessions: 7 blocks for each of the conditions and 4 blocks for each of the conditions. Nine participants completed one long session, five participants completed two long sessions, fourteen participants completed three short sessions and six participants completed four short sessions.

Experiment 3: Block duration: 15 seconds. Interval between blocks: 7 sec. Each condition was repeated eight times per session. Ten participants completed three sessions and twenty-three participants completed two sessions.

Experiment 4: Block duration: 10 seconds. Interval between blocks: 7.5 sec. Two types of sessions: 14 blocks for each of the two conditions and 7 blocks for each of the two conditions. Fourteen participants completed one long session, twelve participants completed two long sessions, eight participants completed one long and one short session.

3. Describe how behavioral performance was measured.

Responses in the fMRI scanner using response box:

Experiment 1: internal experience vividness ratings after each trial (1 ["highest vividness"] to 4 ["lowest vividness"])

Experiment 2: after each trial participants responded according to condition. 1) "self-processing" condition: to decide whether the action described by a verb was characteristic or not of a participant; 2) "non-self-processing" condition: to decide whether an action was characteristic of some ideal person; 3) "letters comparison" condition: to compare the third and fourth letters based on their alphabetic order; this condition was included for another study and was not reported here.

Experiment 3: to press one of the buttons on the response box when the same image appeared twice in a row (i.e., "1-back task").

Experiment 4: to press on any button of a response box when last and first words (non-words) of the sentence (non-word series) were the same (i.e., "1-back task").

Behavioral assessment outside the scanner (questionnaires) :

Rating of the subjective experiences during scanning [Likert scale: 1 (low level)–10 (high level)].

Regarding Experiment 2: "To what extent each one of the tasks was associated with self-related and personal thoughts?"

Regarding Experiment 1 & 2: "To what extent each one of the tasks was associated with having a mental scene in your mind?"

## ► Acquisition

4. Imaging

a. Specify the type(s) of imaging.

functional (4 experiments) and anatomical (T1)

b. Specify the field strength (in Tesla).

3 Tesla

c. Provide the essential sequence imaging parameters.

functional: TR: 2.5 sec; TE: 30 ms; flip angle: 90; slice thickness: 3.6 mm, no gap; FOV: 200 mm; number of slices: 32; data were acquired using a 96x96 matrix (in-plane resolution 2.08x2.08 mm), reconstructed into a 128x128 matrix (in-plane resolution 1.56x1.56 mm).

anatomical: 1x1x1 mm resolution, TE=3.52 ms, TR=9.104 ms

d. For diffusion MRI, provide full details of imaging parameters.

N/A

5. State area of acquisition.

full coverage of cerebral cortex

## ► Preprocessing

6. Describe the software used for preprocessing.

SPM5 (Wellcome Trust Centre for Neuroimaging, London, UK; <http://www.fil.ion.ucl.ac.uk>)

7. Normalization

a. If data were normalized/standardized, describe the approach(es).

A unified segmentation procedure (Ashburner and Friston, 2005) was used for normalization.

b. Describe the template used for normalization/transformation.

SPM5 T1 template

8. Describe your procedure for artifact and structured noise removal.

Standard SPM artifact removal procedure: realignment, slice-time correction, motion correction

9. Define your software and/or method and criteria for volume censoring, and state the extent of such censoring.

Data of participants with excessive movements in the scanner (>1 cm) were excluded (5 participants).

## ► Statistical modeling & inference

10. Define your model type and settings.

For each of four experiments the first-level fixed effects GLM model (boxcar function) was estimated. Six motion parameters from preprocessing step were included as the covariate of no interest. Second-level random effects group models were estimated using first-level contrasts.

11. Specify the precise effect tested.

GLM:  
 Experiment 1: contrasts between each of four internal tasks vs. "rhyme-generation" condition (contrasts 1-4)  
 contrast between four internal tasks combined vs. "rhyme-generation" (contrast 5)  
 Experiment 2: contrast between "self-processing" vs. "non-self-processing" conditions (contrast 6)  
 Experiment 3: contrast between "scenes" vs. "objects" conditions (contrast 7)  
 Experiment 4: contrast between "sentences" vs. "non-words" conditions (contrast 8)

Representational similarity analyses:

Between contrast 5 and contrast 6  
 Between contrast 5 and contrast 7  
 Between contrast 5 and contrast 8  
 Between contrast 6 and contrast 7  
 Between contrast 6 and contrast 8  
 Between each of contrasts 1-4 and contrast 6  
 Between each of contrasts 1-4 and contrast 7  
 Between each of contrasts 1-4 and contrast 8

12. Analysis

- a. Specify whether analysis is whole brain or ROI-based.

Both whole brain and ROI analyses

- b. If ROI-based, describe how anatomical locations were determined.

ROIs were defined individually for each participant as the cluster with the highest DMN selectivity in the first session. Data used for ROI definition (session 1) were not used in the main analysis. ROIs were created automatically (MATLAB custom code) based on the individual DMN peak activations constrained by the parcellation atlas of Craddock and colleagues (Craddock et al., 2012).

13. State the statistic type for inference.  
(See [Eklund et al. 2016.](#))

The resulting activation maps were thresholded with a voxel-wise primary threshold  $p\text{-value} < 0.001$  and cluster-level threshold  $p\text{-value} < 0.05$ , corrected. The primary threshold  $p\text{-value} < 0.001$  has been previously shown to control well for the false positive rate (Woo et al., 2014; Eklund et al., 2016). The cluster-level thresholding was done using Monte-Carlo simulation using the AlphaSim function in a REST toolbox (Song et al., 2011).

14. Describe the type of correction and how it is obtained for multiple comparisons.

see item above

15. Connectivity

- a. For functional and/or effective connectivity, report the measures of dependence used and the model details.

N/A

- b. For graph analysis, report the dependent variable and functional connectivity measure.

N/A

16. For multivariate modeling and predictive analysis, specify independent variables, features extraction and dimension reduction, model, training and evaluation metrics.

N/A